

REINHOLD ENVIRONMENTAL Ltd.



## **2014 NO<sub>x</sub>-Combustion Round Table & Expo Presentations**

February 10 & 11, 2014, in Charlotte, NC / Hosted by Duke Energy

All presentations posted on this website are copyrighted by Reinhold Environmental, Ltd (RE). Any unauthorized downloading, attempts to modify or to incorporate into other presentations, link to other websites, or obtain copies for any other uses than the training of attendees to RE's Conferences is expressly prohibited, unless approved in writing by RE or the original presenter. RE does not assume any liability for the accuracy or contents of any materials contained in this library which were presented and/or created by persons who were not employees of RE.

---

---

# Low and High Temperature Corrosion Associated with Pollutant Control Technologies



Kevin Davis

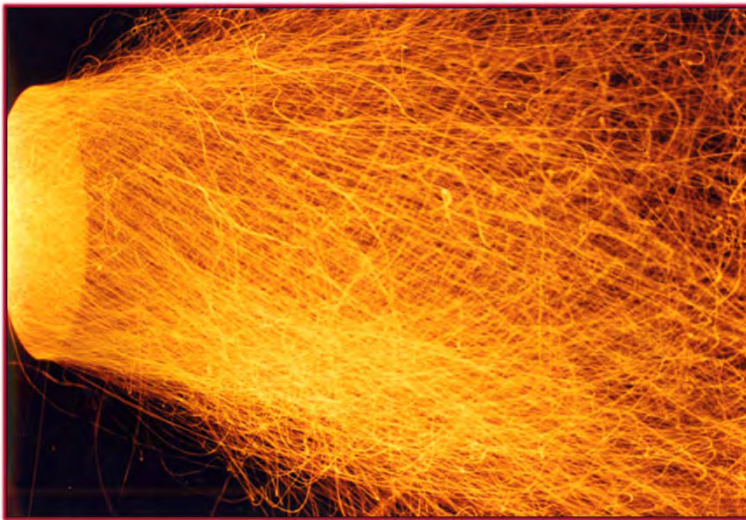
Vice President, Process Evaluation & Testing



# Reaction Engineering International

---

- ➔ Privately held consulting firm recognized for independent analysis and evaluations involving a range of industrial combustion applications

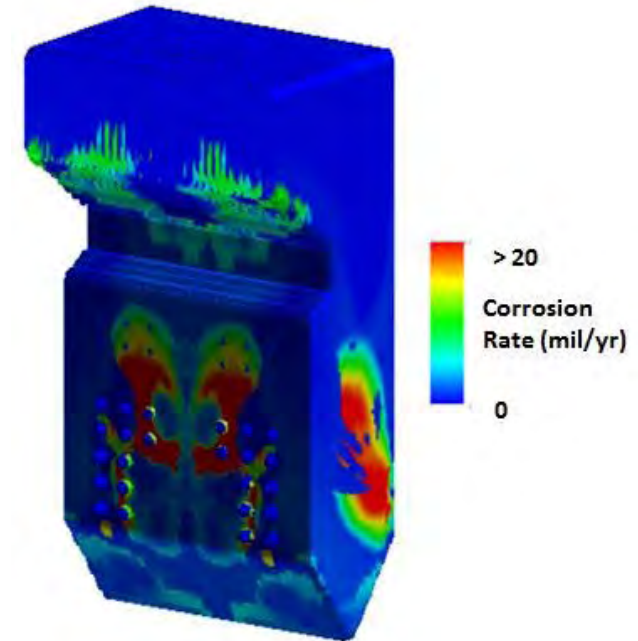


- ➔ Technical focus on multi-phase, chemically reacting flows
- ➔ Serving the utility industry since 1990
- ➔ Affiliates in Asia and Europe
- ➔ Established capabilities include advanced modeling and testing

# REI Coal-Fired Boiler Corrosion Experience

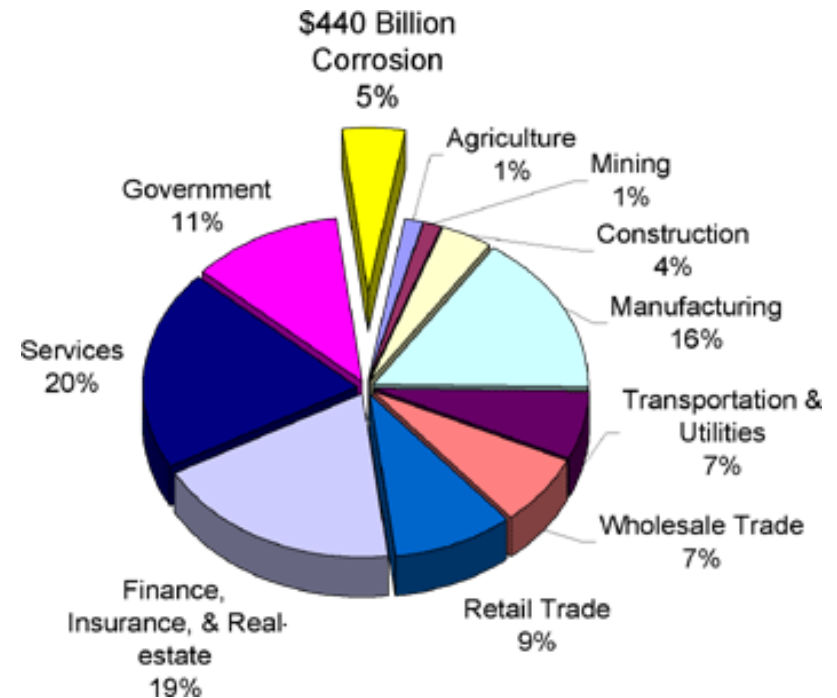
---

- ➔ Efforts focused on impacts of firing system modifications, fuel changes, additive utilization, and operational optimization
- ➔ CFD-based modeling
  - ◆ Correlation-based approach resulting from collaborations with EPRI and KEPRI
  - ◆ Integrated with REI's CFD software (*GLACIER*)
- ➔ Real-time monitoring
  - ◆ Initially motivated by desire to validate modeling tools
  - ◆ Adaptation of an electrochemical approach in a collaborative effort with Corrosion Management (UK)



# Impact of Corrosion

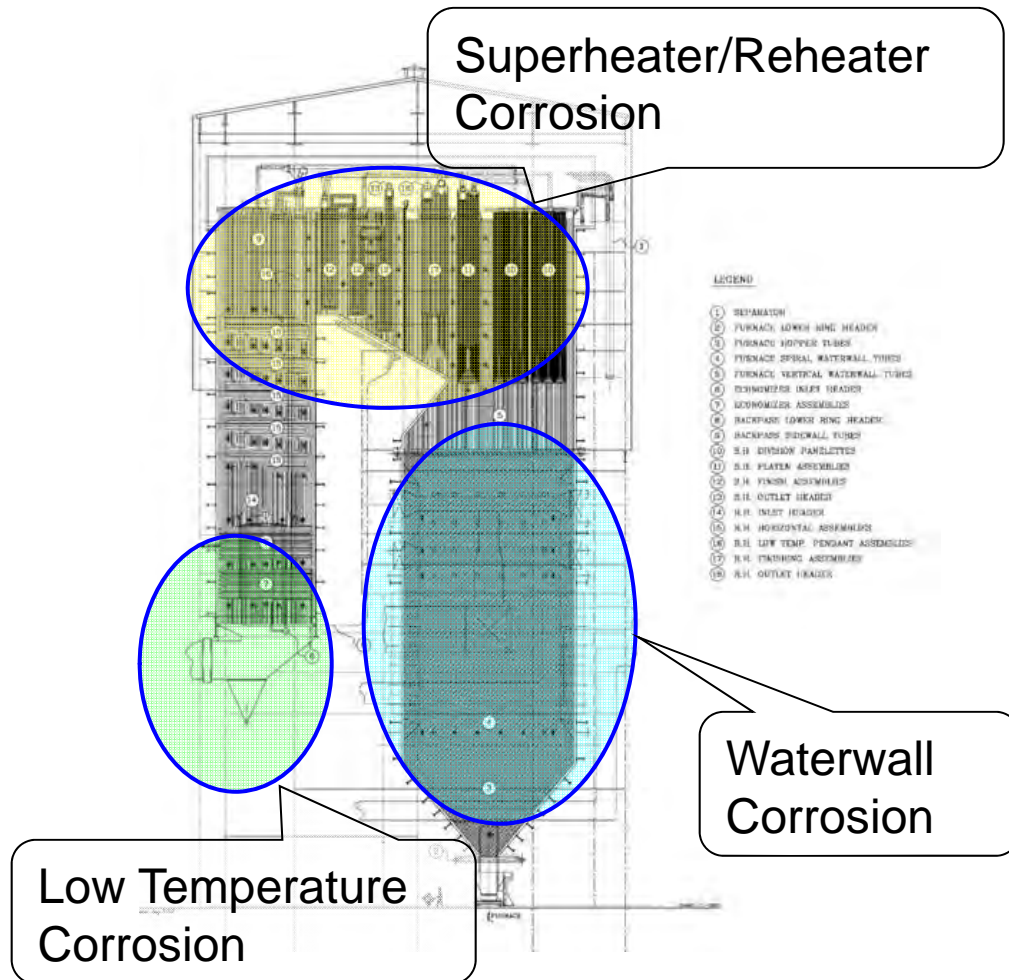
- ➔ Overall US Economic Impact: \$440 billion/yr or 5% of GDP (Federal Highway Administration)
- ➔ Large impact on the US Electric Power Industry
- ➔ Economic and environmental pressures are increasing corrosion challenges:
  - ◆ NO<sub>x</sub> / Hg emissions
  - ◆ Fuel cost and availability
  - ◆ Generation efficiency
  - ◆ Opportunity fuels
  - ◆ CO<sub>2</sub> separation



***“Corrosion costs the U.S. electric power industry up to \$10 billion per year and is the cause of roughly half of the forced outages in steam generating plants.”***

**EPRI, 1998**

# Fireside Corrosion



- ➔ High temperature corrosion of waterwalls
- ➔ High temperature corrosion of superheater/reheater
- ➔ Low temperature corrosion of economizer
- ➔ Low temperature corrosion of air preheater

---

---

# Waterwall Corrosion

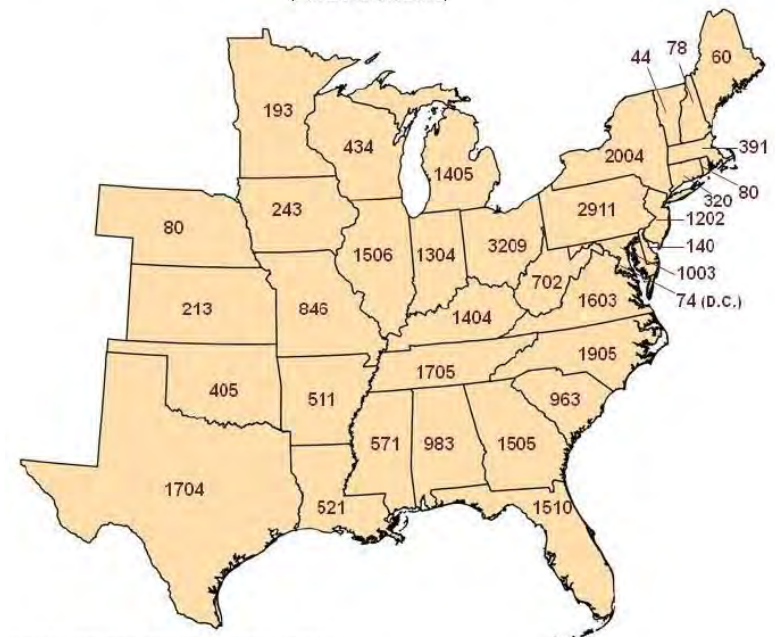
---

---

# NOx Regulations

- Clean Air Act of 1970 and subsequent amendments (1990) required substantial reductions in NOx emissions from coal power plants
- Cross State Air Pollution Rule tightens limits on NOx in 28 eastern states
- CSAPR vacated Aug 2012, full court review denied Jan 2013, Clean Air Interstate Rule in effect until satisfactory replacement rule is developed by EPA
- Regional haze regions near 156 national parks/wilderness areas

New Power Plant Emission Standards for Eastern States  
Estimated Lives Saved Each Year Beginning in 2014  
(PM 2.5 and Ozone)



Data Source: EPA, Regulatory Impact Analysis

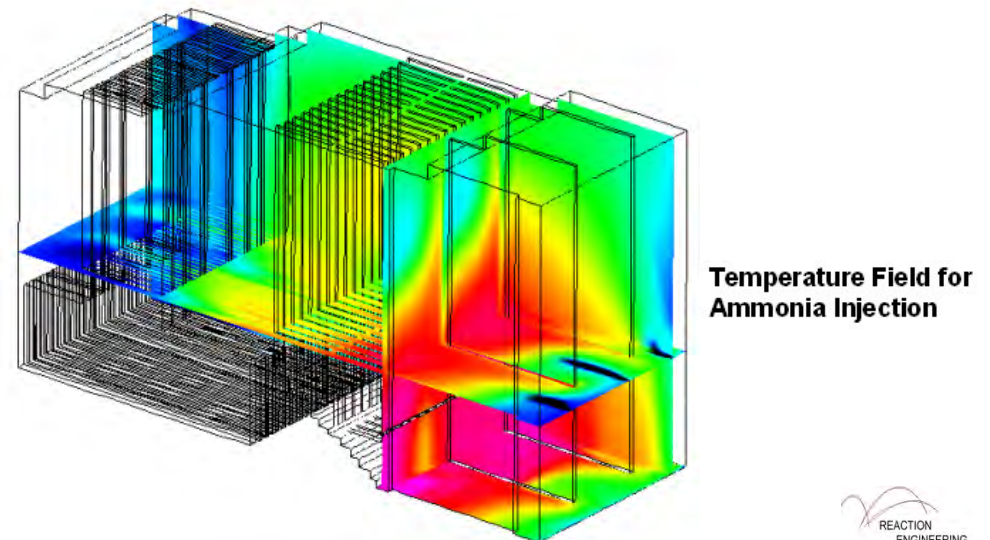
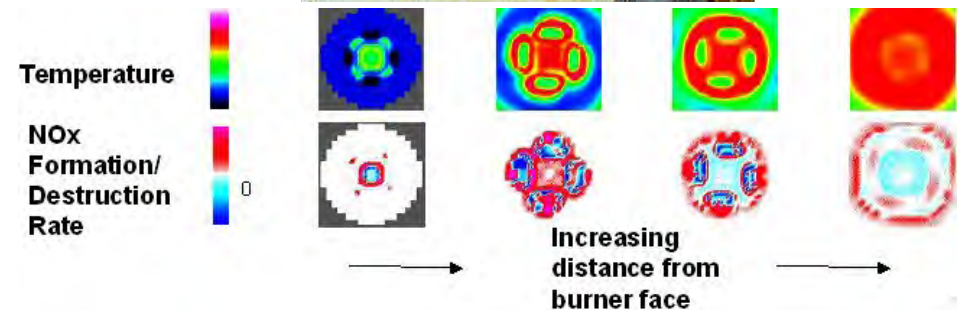
# NOx Control Strategies

## → Technology experience

- Low NOx burners
- Over-fire air
- Fuel switching and blending/co-firing
- Traditional Gas/coal and fuel-lean-gas reburning
- Amine reagent injection (SNCR, advanced reburn, rich reagent injection)
- SCR

## → Operational Impacts

- Carbon-in-ash
- Waterwall wastage
- Heat balance
- CO emissions
- Deposition and ash loading
- Ammonia slip
- Soot formation



# Corrosion and Coal-fired Boilers

## → Environmental and Economic Pressures vs. Corrosion

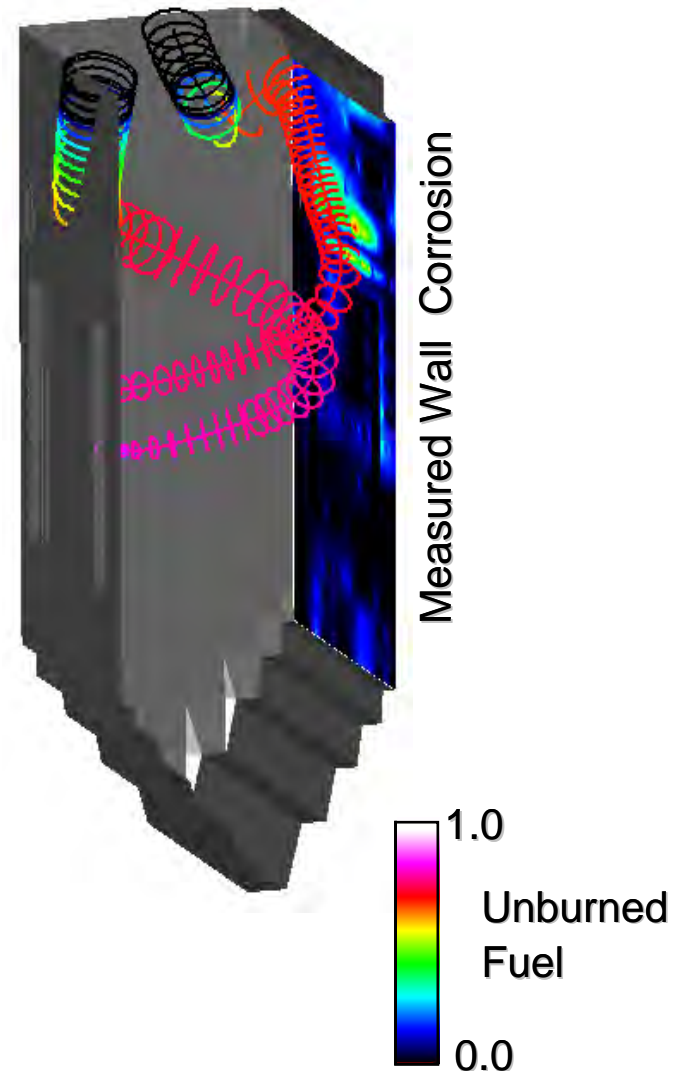
- ◆ NO<sub>x</sub> emissions
- ◆ Fuel cost and availability
- ◆ Steam temperatures

## → Sulfur Mechanism

- ◆ Combustion modifications for NO<sub>x</sub> control
- ◆ Supercritical steam cycle
- ◆ High sulfur content fuel

## → Chlorine Mechanism

- ◆ Combustion modifications for NO<sub>x</sub> control
- ◆ High heat flux to water-walls
- ◆ High chlorine content fuel



# Corrosion Mechanisms

---

- ➔ Tube wall interaction with gaseous phase constituents
  - ◆ Under oxidizing conditions metal loss is very slow and a protective  $\text{Fe}_3\text{O}_4$  scale forms
  - ◆ Under reducing conditions, reducing sulfur species or fuel chlorine may disrupt the protective scale and metal loss occurs
  
- ➔ Tube wall interaction with deposit
  - ◆ Pyrite ( $\text{FeS}_2$ ) in coal is converted to FeS
  - ◆ Metal loss may occur in areas where unoxidized material, especially FeS, is deposited
  
- ➔ Highest wastage rates are due to tube wall interaction with chlorine and FeS deposits – up to 100 mil/yr or more

# Corrosion Modeling Approach

---

- ➔ Development of advanced corrosion correlations (models) for three corrosion mechanisms
  1. Gas phase attack by reduced sulfur species such as  $H_2S$
  2. Deposition of unreacted fuel and resulting sulfur-based attack
  3. Chlorine-based attack
- ➔ Incorporation of these correlations into two-phase, reacting CFD code
- ➔ Validation of the correlations through pilot-scale tests and CFD simulations

# Corrosion Due to Gaseous Sulfur Species

---

- Sulfidation of metal primarily due to interaction with gaseous phase  $H_2S$ , also  $CS_2$  &  $COS$
- Corrosion rates are low
- Kung's correlation (Material Performance, (36)36-40 (1997))

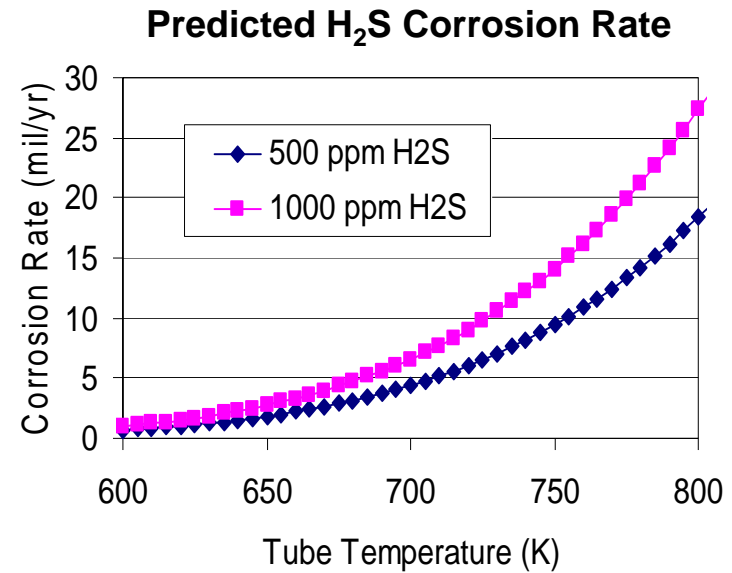
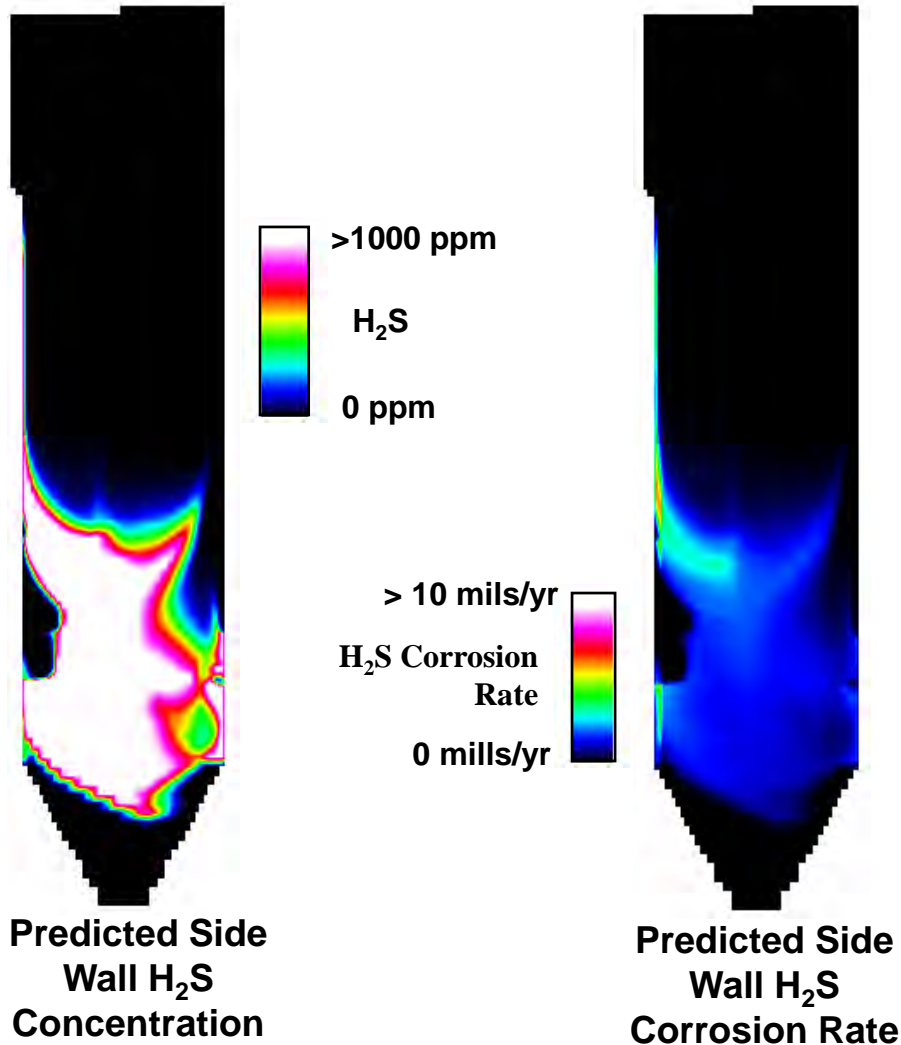
- ◆ For low alloy steels ( $Cr\% < 10\%$ ):

$$CR = 3.2 \times 10^5 \exp\left(-\frac{15,818}{1.987T}\right) \times [H_2S]^{0.574} \times \frac{1}{(Cr\% + 10.5)^{1.234}} \pm 2.2$$

- ◆ For high chromium steels ( $10\% < Cr\% < 16\%$ ):

$$CR = 1.04 \times 10^7 \exp\left(-\frac{19,230}{1.987T}\right) \times [H_2S]^{0.29} \times \frac{1}{(Cr\% + 1.40)^{1.37}} \pm 1.2$$

# Predicted H<sub>2</sub>S Corrosion in a Wall-Fired Furnace



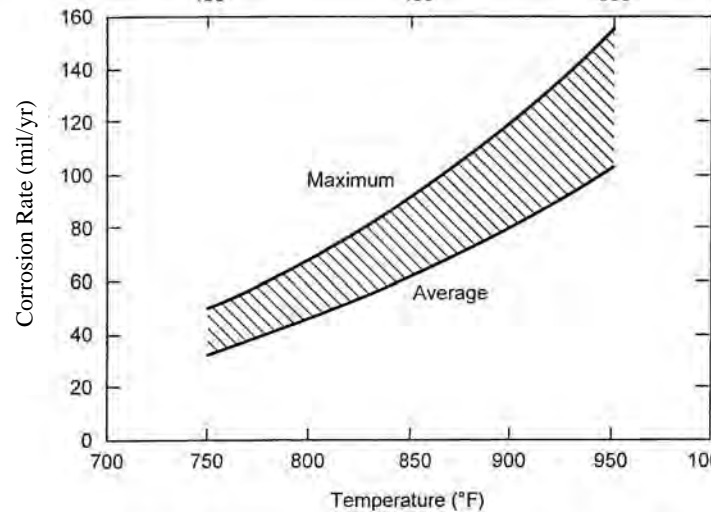
- H<sub>2</sub>S corrosion alone cannot account for observed high corrosion rates (up to ~100 mil/yr), even at  $T_{\text{tube}} = 750$  K

# Corrosion Due to Deposition of FeS & Carbon

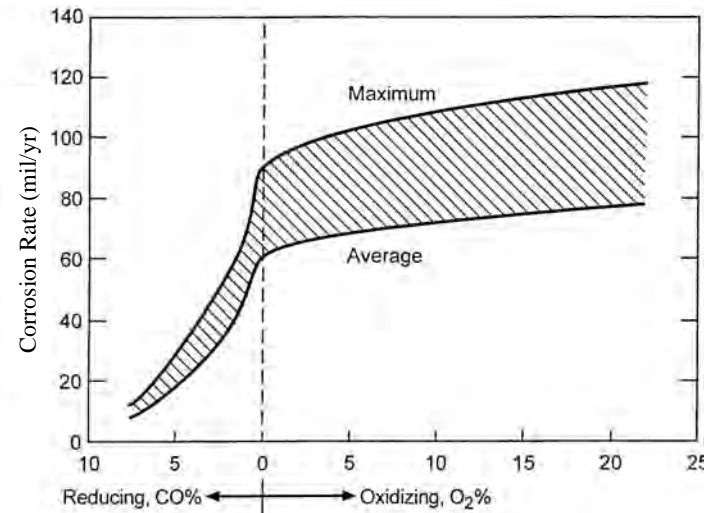
---

- ➔ Corrosion may occur where unoxidized FeS and coal are deposited
- ➔ Deposit based corrosion is associated with a high fraction of unoxidized material in deposit, high tube temperatures, high heat flux
- ➔ Experimental evidence indicates that the highest corrosion rates occur when unoxidized deposits are exposed to oxidizing flue gas

# EPRI Experimental Work



Corrosion rate under FeS deposit as a function of temperature in a 1% O<sub>2</sub> environment.



Corrosion rate under FeS deposit as a function of gas O<sub>2</sub> and CO content at 450°C.

EPRI experimental work for metal under an FeS layer:

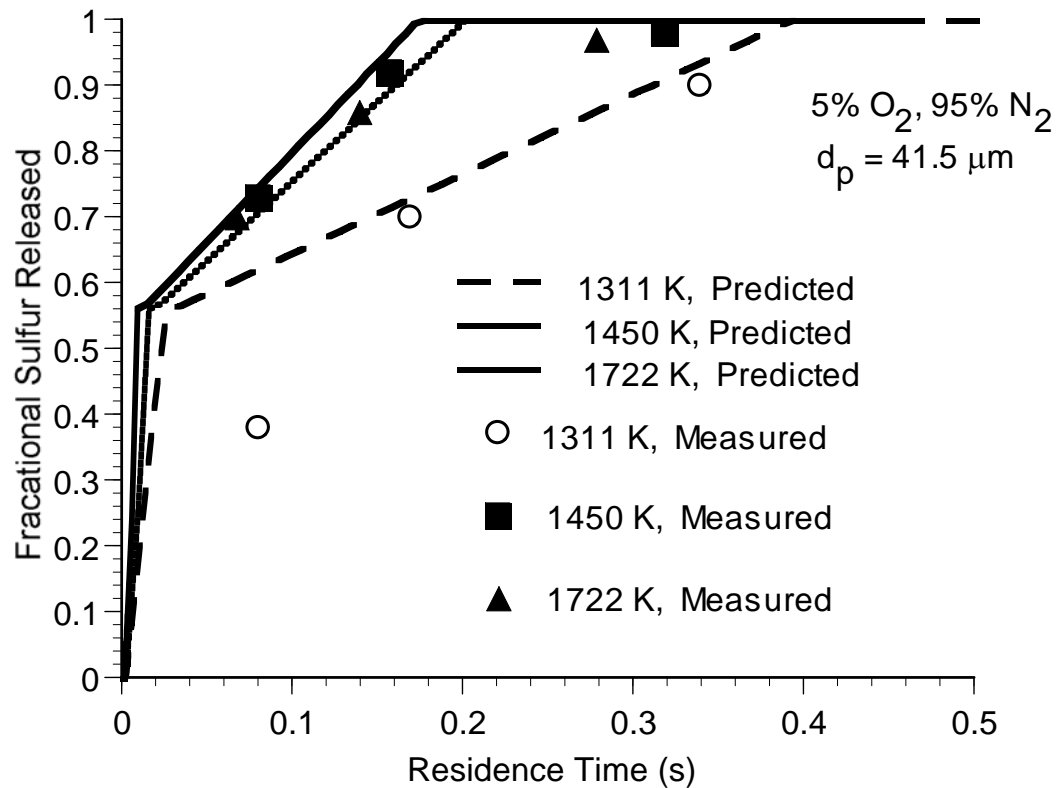
- ◆ Very high corrosion rates may occur
- ◆ Corrosion rates increase with temperature
- ◆ Corrosion rates are highest under oxidizing or mildly reducing conditions

# Predicting Waterwall Deposition of Coal Sulfur

---

- ➔ Included sulfur: pyrite ( $\text{FeS}_2$ ) and organic sulfur bound within the coal particle matrix
  - ◆ Tracked with the coal particles
  - ◆ Wall deposition predicted by particle wall impaction/deposition modeling
  
- ➔ Excluded pyrite: pyrite particles
  - ◆ Different density, particle size distribution, and kinetics than coal
  - ◆ Model of Srinivasachar and Boni model for pyrite kinetics (*Fuel*, 1989) has been included in *GLACIER*
    - » Thermal decomposition of pyrite ( $\text{FeS}_2$ ) to pyrrhotite ( $\text{Fe}_{0.877}\text{S}$  or  $\text{FeS}$ ) at 870 K (~1100 F) – occurs quickly
    - » Oxidation of pyrrhotite ( $\text{Fe}_{0.877}\text{S}$ ) to magnetite ( $\text{Fe}_3\text{O}_4$ ) – occurs more slowly

# Excluded Pyrite Kinetics: Model vs Measurement



- Model shows the initial fast thermal decomposition from FeS<sub>2</sub> to FeS<sub>0.877</sub> followed by slower oxidation of FeS<sub>0.877</sub>
- Sulfur evolution is faster at higher temperature
- Model predictions agree with measurements

Data from Levasseur et al., 1989

## Effect of Temperature

# Prediction of Corrosion Due to FeS Deposition

---

- Based on curve fit of published data

$$CR = A \times f(S) \times h(dep) \times g(SR) \times e^{-\left(\frac{Q_r}{RT}\right)}$$

$CR$  = corrosion rate in mil/yr

$f(S)$  is a linear function from 0 to 1 of the coal sulfur content  $S$ , reaching 1 for  $S = 1\%$

$h(dep)$  is a linear function from 0 to 1 of the fraction of unoxidized material in the total material deposited  $dep$ , reaching 1 at  $dep = 0.2$

$Q_r = 10313$  cal/mol

$R = 1.987$  cal/K/mol

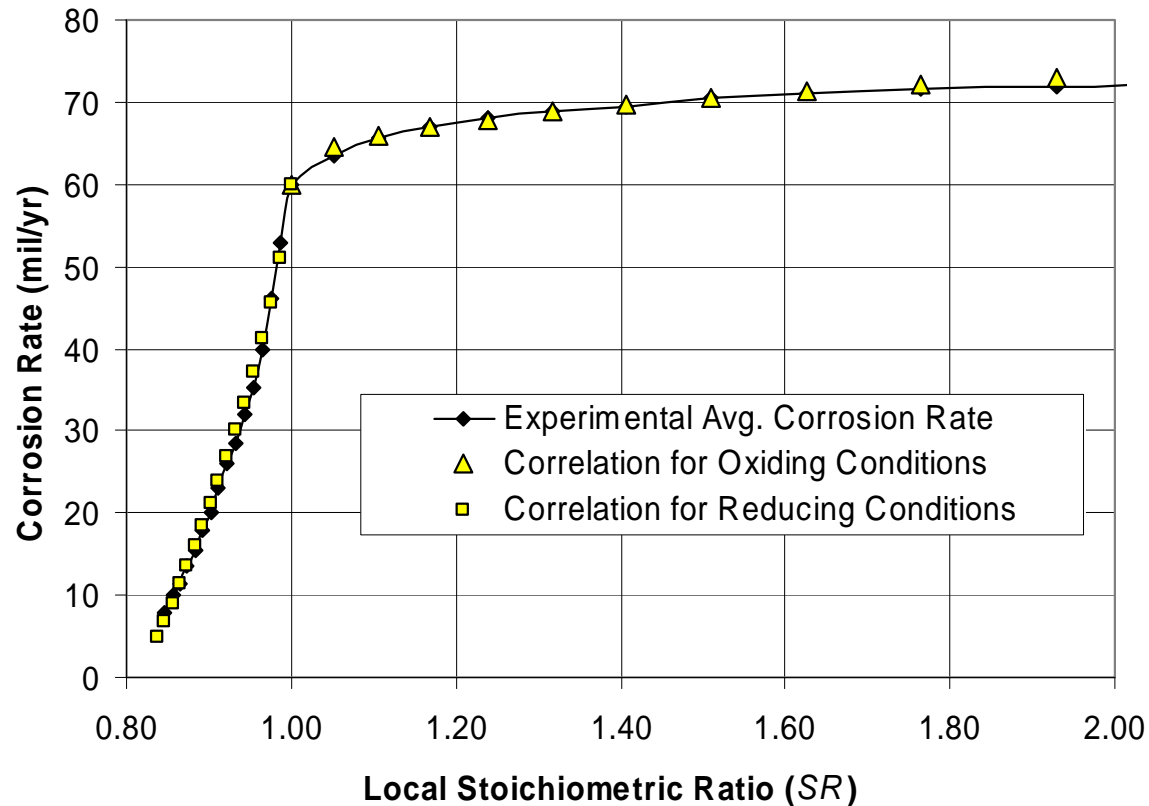
$A = 1174$

$g(SR) = -197.6 \times (1-SR)^{0.7} + 60$  for reducing conditions where  $SR \leq 1$

or

$g(SR) = 13.4 \times (SR-1)^{0.37} + 60$  for oxidizing conditions where  $SR \geq 1$

# Predicted Corrosion Rates vs Measurements

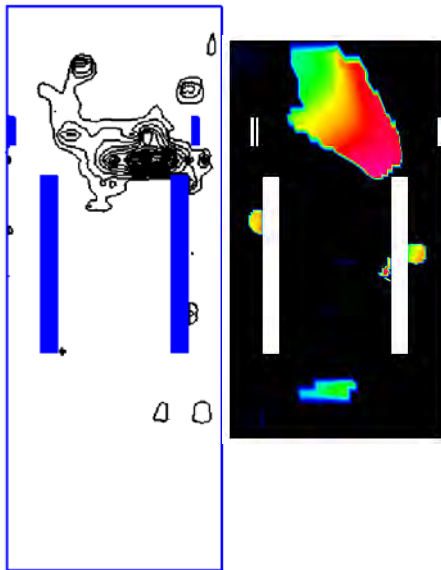


➤ Predicted corrosion rate as a function of stoichiometric ratio (SR) at 450° C. compares well with EPRI experimental data

**Corrosion rate correlation vs. experimental data as a function of the local stoichiometric ratio (SR) for constant T = 450° C.**

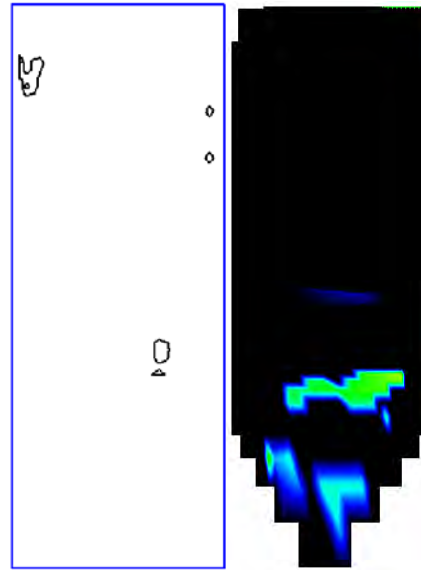
# Validation Using Plant UT Data

Rear Wall



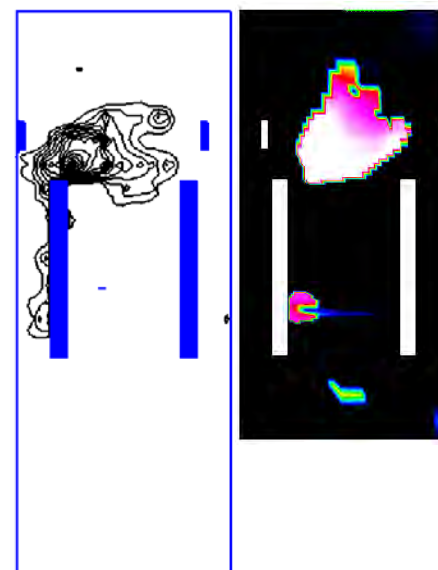
(max = 81 mil/yr)

Side Wall



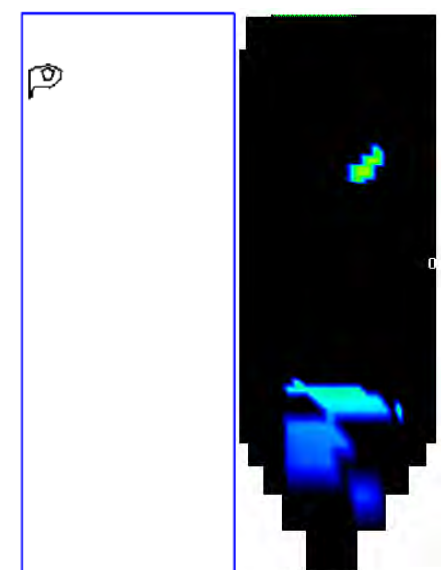
(max = 26 mil/yr)

Front Wall

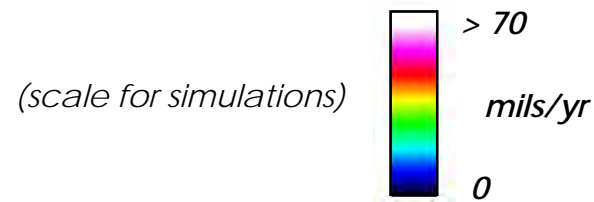


(max = 94 mil/yr)

Center Wall



(max = 29 mil/yr)



# Corrosion due to Chlorine

---

---

- ➔ Well documented in the UK due to the relatively high chlorine content of UK coals
- ➔ Often associated with high fuel chlorine content ( $> 0.15\%$ ) and flame impingement
- ➔ Corrosion has not been consistently observed with high chlorine coal
- ➔ More recently observed in the U.S. in a few boilers using high chlorine coals

# Chlorine Corrosion Conditions and Mechanisms

---

---

- Observed in presence of high heat flux, fuel-rich regions when fuel chlorine > 0.15%
- FeCl<sub>2</sub> forms at the metal surface, breaks up protective scale
- Complex interactive behavior in the presence of sulfur based on reducing and oxidizing conditions
- Davis et al. correlation (Material Science Forums, (369-372) 857-864 (2001)

$$CR = (C \times \% Cl) \times (HF)^m \times \exp\left(-\frac{Q_{cl}}{RT}\right) - d$$

# Chlorine Corrosion Correlation

---

---

- Based on curve fit of a published correlation

$$CR = (136.55 \times \%Cl) \times (HF)^{1.725} \times \exp\left(-\frac{12,590}{1.987T}\right) + 9.56$$

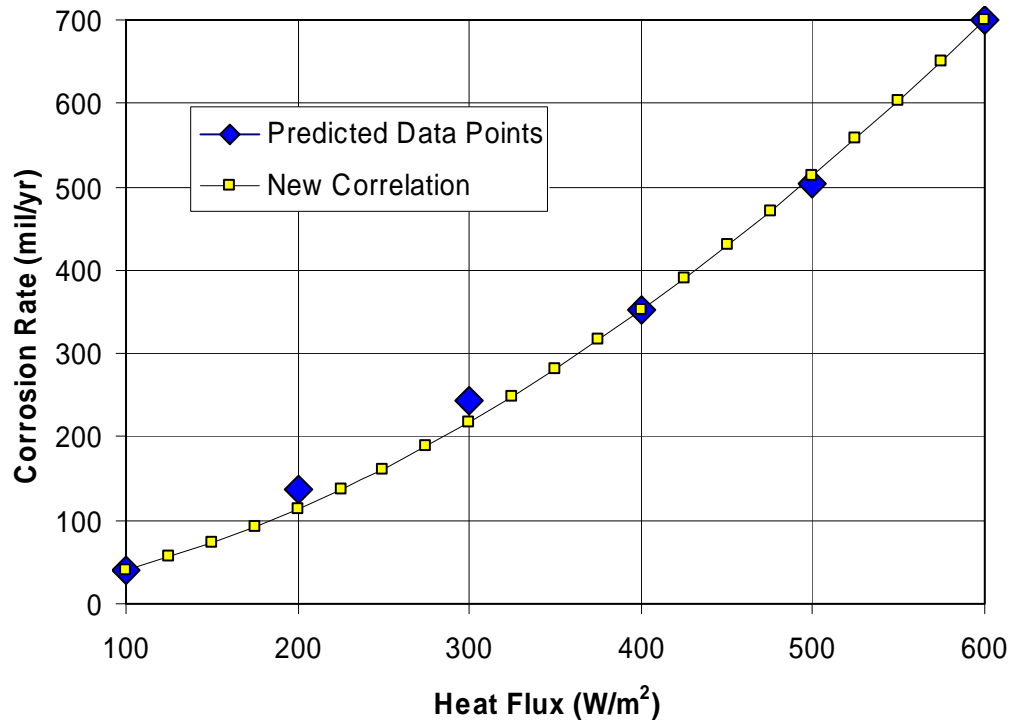
$CR$  = chlorine corrosion rate in mil/yr

$\%Cl$  = weight % coal chlorine content

$T$  = tube metal temperature in Kelvin

$HF$  = wall heat flux in kW/m<sup>2</sup>.

# Chlorine Corrosion Correlation Tuning

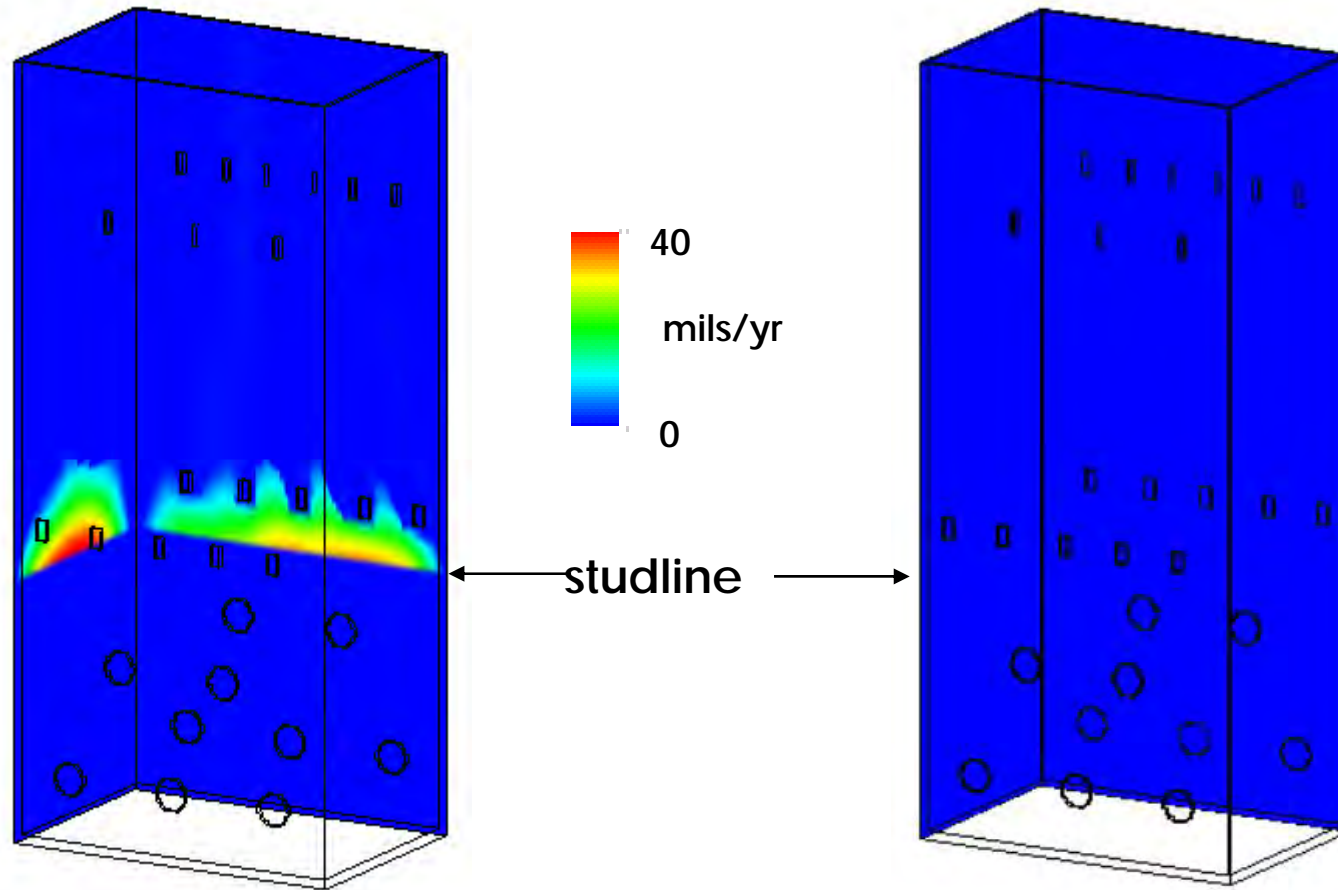


➔ New correlation predicted chlorine corrosion rate is comparable to the experimentally verified predictions of Davis et al (2002)

**Chlorine corrosion correlation vs. predicted data points of Davis et al (2000)**

# Cyclone-fired Boiler Chlorine Corrosion

---



40/60 Bit/PRB

10/90 Bit/PRB

# Waterwall Corrosion

---

## → Gas phase H<sub>2</sub>S Corrosion

$$CR_{H_2S} = a \cdot f_1(T_m) \cdot f_2(Cr\%) \cdot f_3(H_2S) + b$$

## → Deposition of Unoxidized Material

$$CR_{dep} = a \cdot f_1(dep) \cdot f_2(Stoichiometry) \cdot f_3(T_m) + b$$

## → Chlorine-based Corrosion

$$CR_{Cl} = a \cdot f_1(\%Cl) \cdot f_2(HeatFlux) \cdot f_3(T_m) + b$$

---

---

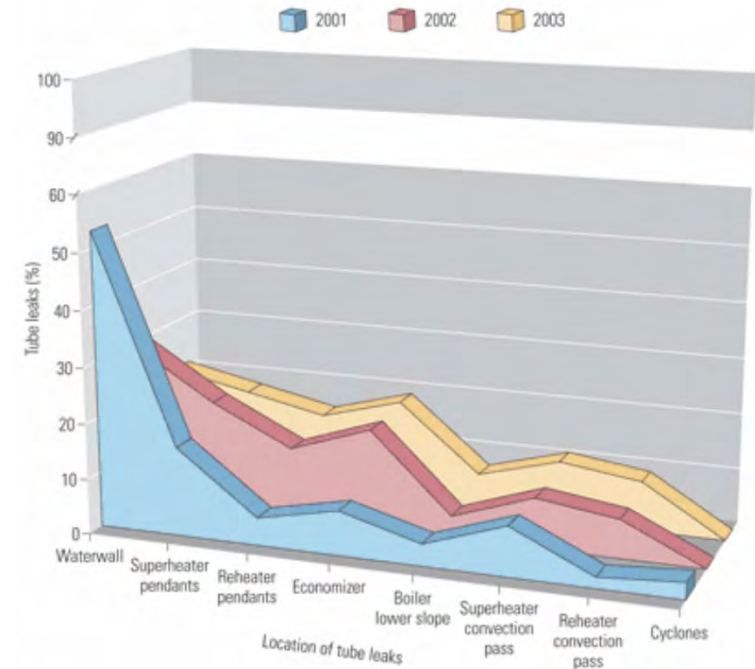
# Superheater/Reheater Corrosion

---

---

# Evolution of Boiler Corrosion

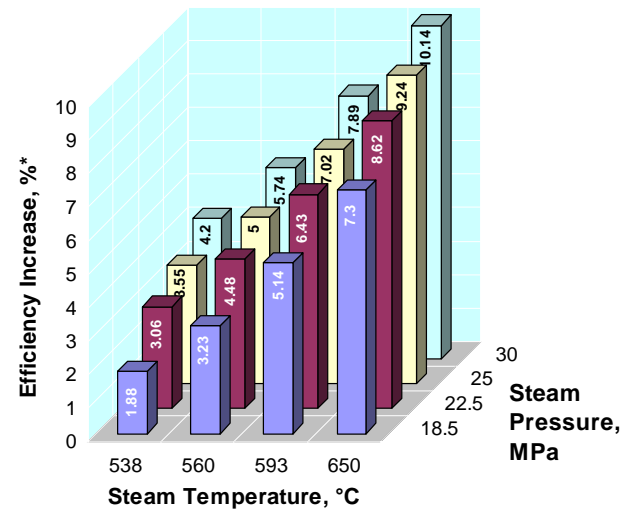
- ➔ Corrosion problems have been identified but not solved, just avoided.
- ➔ 2005 survey reports that more than half of the tube leakage is from corrosion.
- ➔ Corrosion can be enhanced by:
  - ◆ Formation of reducing environment through air staging
  - ◆ Deposition of unburned material
  - ◆ Enhanced steam conditions



*Patrick J, Oldani R, Behren DV, "Benchmarking boiler tube failures – Part 2," Power 149 (9), 55-59, November/December 2005*

# USC and Superheater Corrosion

- Ultra-supercritical plants increase thermal efficiency while reducing carbon consumption
- Enhanced steam pressure and temperature in ultra-supercritical (USC) unit
  - ◆ Current supercritical units: 540°C/16.5-24MPa
  - ◆ Plans for 650°C/34.5MPa
  - ◆ Currently 593°C/27MPa unit is operating
- Additional benefits include reduced emissions of SO<sub>x</sub>, NO<sub>x</sub>, and CO<sub>2</sub>.
- Steam conditions present significant challenges to materials selection

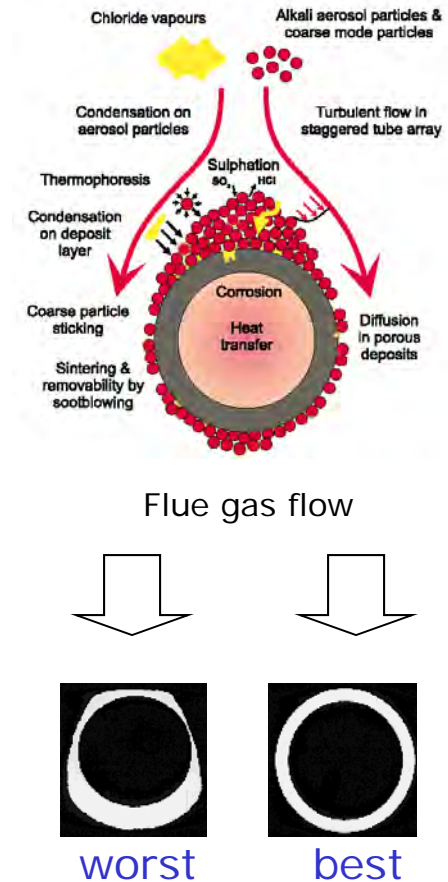


\* Based on 538°C/18.5MPa Single Reheat Case

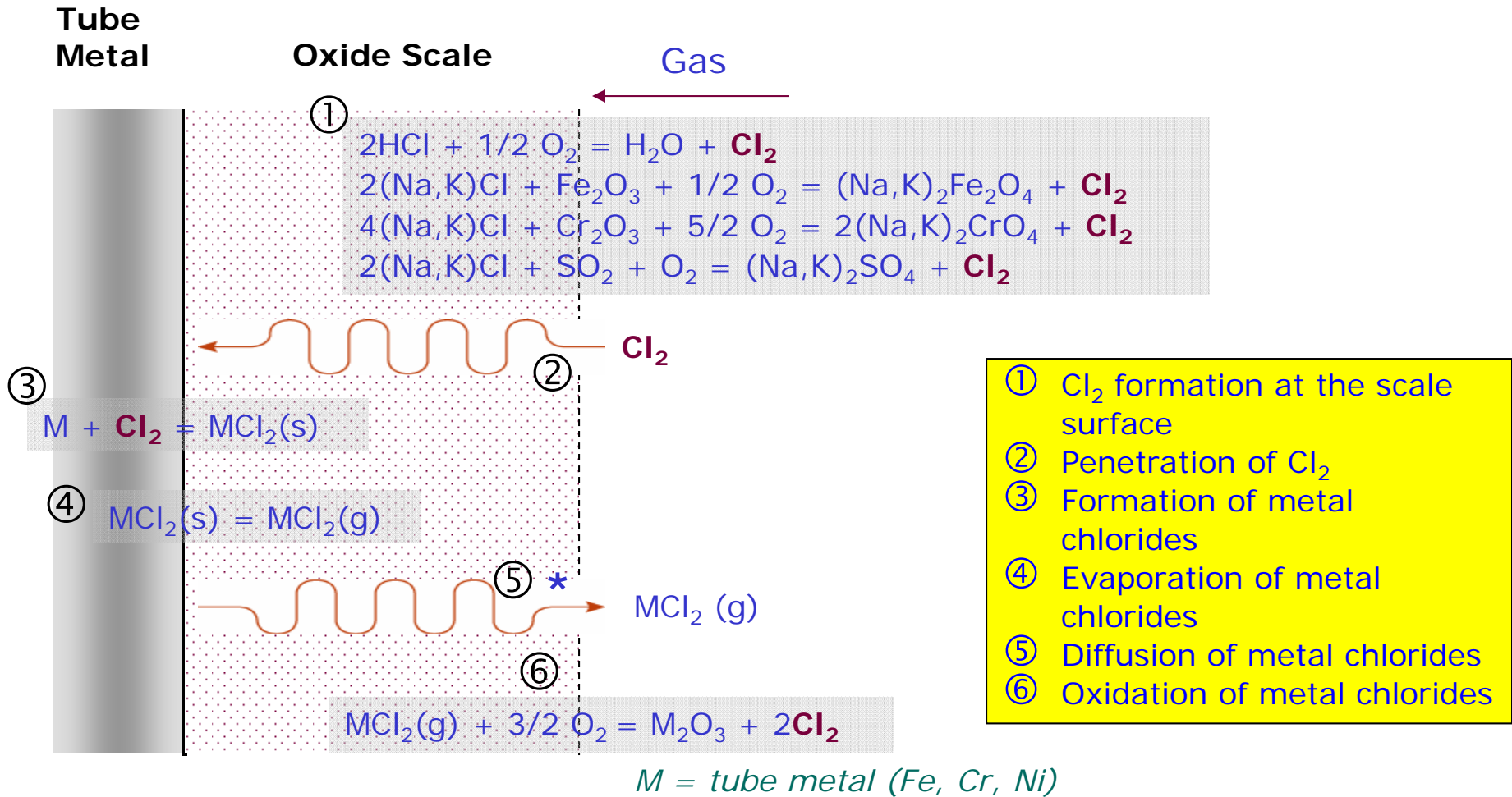
adapted from Viswanathan R, Bakker WT, "Materials for Boilers in Ultra Supercritical Power Plants," Proceedings of 2000 International Joint Power Generation Conference, July 23-26, 2000.

# Major Corrosion Factors

- ➔ Temperature
  - ◆ Metal and Gas Temperature
  - ◆ Heat Flux
  - ◆ Temperature Gradient
  - ◆ Temperature Fluctuations
- ➔ Fuel/Deposit Characteristics
  - ◆ Sulfur, Chlorine, Alkali metal
- ➔ Local Gas-Phase Stoichiometry
- ➔ Tube Metallurgy
  - ◆ Cr, Ni, Al, etc.
- ➔ Boiler Design
  - ◆ tube spacing, tube location, etc.
- ➔ Flue Gas Velocity

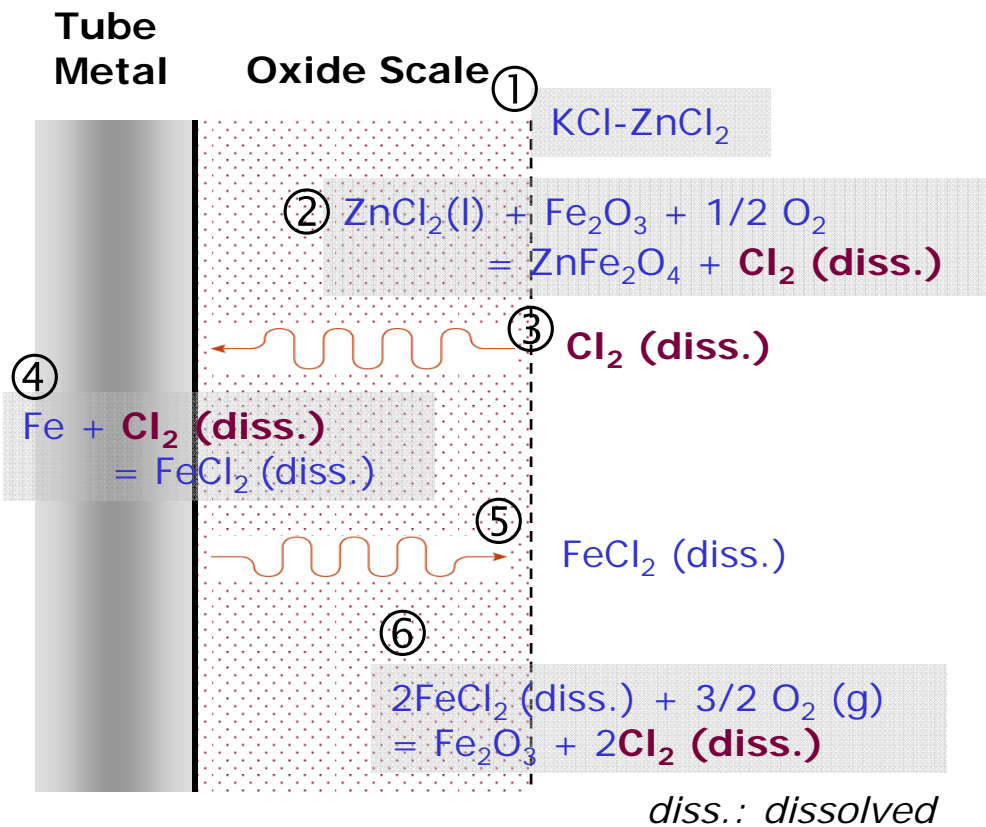


# Active Oxidation



- ①  $Cl_2$  formation at the scale surface
- ② Penetration of  $Cl_2$
- ③ Formation of metal chlorides
- ④ Evaporation of metal chlorides
- ⑤ Diffusion of metal chlorides
- ⑥ Oxidation of metal chlorides

# Molten Chlorides



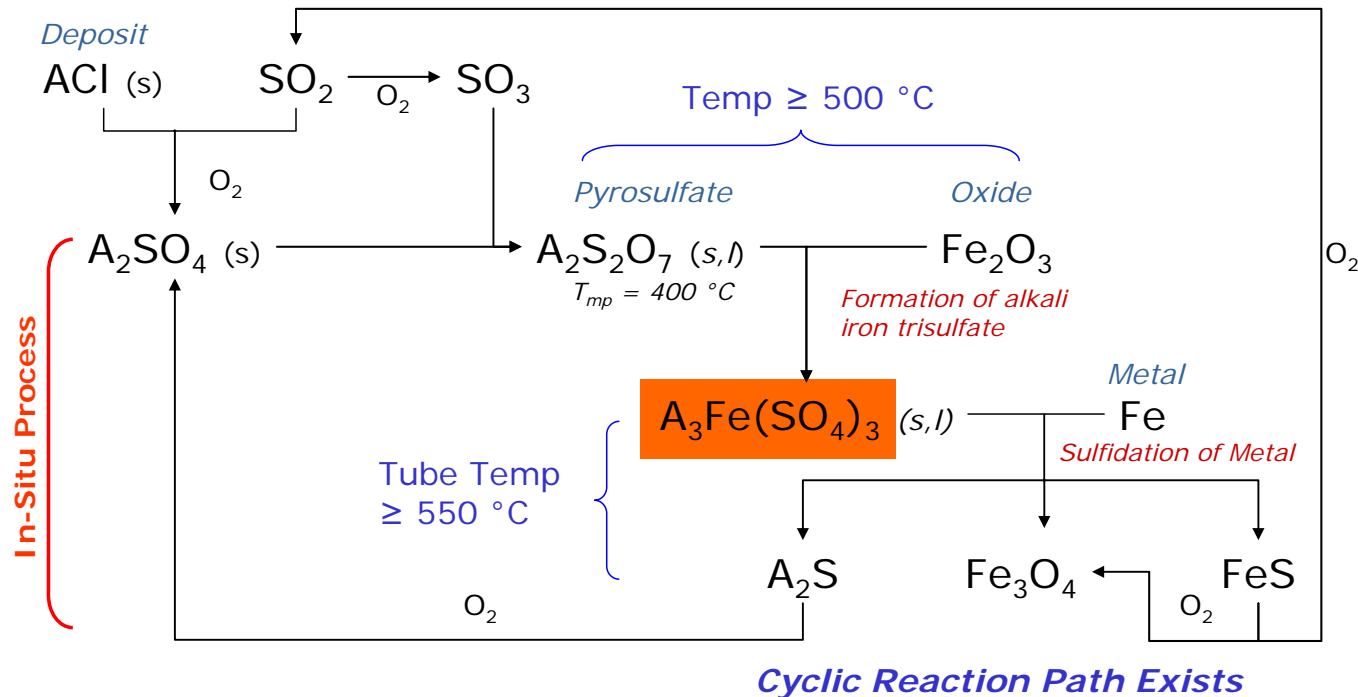
➔ Mixture of chlorides with low melting point (eutectic)

- ◆ M<sub>p</sub> of KCl: 772°C
- ◆ With ZnCl<sub>2</sub> (47% KCl – 53% ZnCl<sub>2</sub>): 355°C

- ① Molten phase formation
- ② Cl<sub>2</sub> (dissolved) formation
- ③ Penetration of Cl<sub>2</sub>
- ④ Metal chloride formation by dissolution
- ⑤ Migration of metal chlorides
- ⑥ Oxidation of metal chlorides

# Coal-ash Corrosion (Molten Sulfate)

A: Alkali Metal (Na or K)



- ➔ Most commonly found superheater corrosion mechanism
- ➔ Corrosion rate shows classical bell-shape as a function of tube temperature based on formation and stability of alkali-metal-trisulfate

# Superheater Corrosion

---

---

## → Active Oxidation

$$CR_{AO} = f_1(T_m) \cdot f_2(Cr\%) \cdot f_3(T_g - T_m) \cdot f_4(Cl\%)$$

## → Molten Sulfate Corrosion

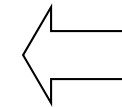
$$CR_{MS} = a \cdot P \cdot HF \cdot f_1(T_m) \cdot f_2(Cr\%) \cdot f_3(\text{Fuel Corrosivity}) \cdot f_4(\text{dep}) + b$$

## → Sulfidation

$$CR_{H_2S} = a \cdot f_1(T_m) \cdot f_2(Cr\%) \cdot f_3(H_2S) + b$$

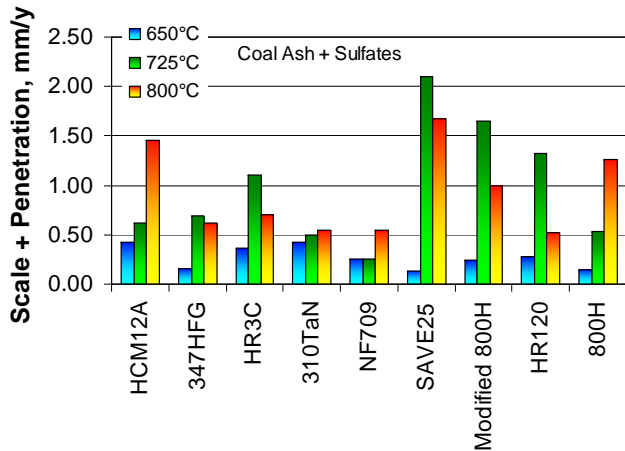
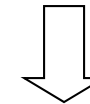
# Candidate Materials for USC

| Group  | Steels         | Specification      |             | Composition, % |       |      |      |      |      |      |      |      |      |      |       |       |      |               |      |
|--------|----------------|--------------------|-------------|----------------|-------|------|------|------|------|------|------|------|------|------|-------|-------|------|---------------|------|
|        |                | ASME               | JIS         | C              | Cr    | Ni   | Co   | Si   | Al   | W    | Cu   | Mo   | Nb   | Mn   | V     | B     | N    | Ti            | Misc |
| 1.25Cr | T11            | T11                |             | 0.15           | 1.25  |      |      | 0.50 |      |      |      | 0.50 |      | 0.45 |       |       |      |               |      |
|        | NFIH           |                    |             | 0.12           | 1.25  |      |      |      |      |      | 1.00 | 0.07 |      | 0.20 |       |       |      |               |      |
| 2Cr    | T22            | T22                | STBA24      | 0.12           | 2.25  |      |      | 0.30 |      |      |      | 1.00 |      | 0.45 |       |       |      |               |      |
|        | HCM2S          | T23                | STBA24J1    | 0.06           | 2.25  |      |      | 0.20 |      | 1.60 |      | 0.10 | 0.05 | 0.45 | 0.25  | 0.00  |      |               |      |
|        | Tempaloy F-2W  |                    |             |                | 2.00  |      |      |      |      | 1.00 |      | 0.60 | 0.05 |      | 0.25  |       |      |               |      |
| 9Cr    | T9             | T9                 | STBA26      | 0.12           | 9.00  |      |      | 0.60 |      |      |      | 1.00 |      | 0.45 |       |       |      |               |      |
|        | HCM9M          |                    | STBA27      | 0.07           | 9.00  |      |      | 0.30 |      |      |      | 2.00 |      | 0.45 |       |       |      |               |      |
|        | T91            | T91                | STBA28      | 0.10           | 9.00  | 0.80 |      | 0.40 |      |      |      | 1.00 | 0.08 | 0.45 | 0.20  |       | 0.05 |               |      |
|        | T92            | T92                |             | 0.07           | 9.00  |      |      | 0.06 | 1.80 |      |      | 0.50 | 0.05 | 0.45 | 0.20  | 0.004 | 0.06 |               |      |
| 12Cr   | E911           |                    |             | 0.12           | 9.00  | 0.25 |      | 0.20 | 0.90 |      |      | 0.94 | 0.06 | 0.51 | 0.20  |       | 0.06 |               |      |
|        | HT91           | (DIN x20CrMoV121)  |             | 0.20           | 12.00 | 0.50 |      | 0.40 |      |      |      | 1.00 |      | 0.60 | 0.25  |       |      |               |      |
|        | HT9            | (DIN x20CrMoWV121) |             | 0.20           | 12.00 | 0.50 |      | 0.40 |      | 0.50 |      | 1.00 |      | 0.60 | 0.25  |       |      |               |      |
|        | Tempaloy F-12M |                    |             |                | 12.00 |      |      |      | 0.70 |      | 0.70 |      |      |      |       |       |      |               |      |
|        | HCM12          |                    | SUS410J2 TB | 0.10           | 12.00 | 0.30 |      | 0.30 | 1.00 | 0.90 | 1.00 | 0.05 | 0.55 | 0.25 |       | 0.03  |      |               |      |
|        | TB12           |                    |             | 0.08           | 12.00 | 0.10 |      | 0.05 | 1.80 |      | 0.50 | 0.05 | 0.50 | 0.20 | 0.30  | 0.05  |      |               |      |
|        | HCM12A         | T122               | SUS410J3 TB | 0.10           | 12.00 | 0.30 |      | 0.30 | 2.00 | 0.90 | 0.40 | 0.05 | 0.50 | 0.20 |       | 0.05  |      |               |      |
|        | NF12           |                    |             | 0.08           | 11.00 |      | 2.50 | 0.20 | 2.60 |      | 0.20 | 0.07 | 0.50 | 0.20 | 0.004 | 0.05  |      |               |      |
| SAVE12 |                |                    | 0.10        | 11.00          |       | 3.00 | 0.30 | 3.00 |      |      |      | 0.20 | 0.20 |      | 0.04  |       |      | 0.07Ta 0.04Nd |      |



Ferritic

Austenitic



| Group         | Specification    |             | Composition, % |       |       |       |      |      |      |      |      |      |      |      |       |       |      |              |
|---------------|------------------|-------------|----------------|-------|-------|-------|------|------|------|------|------|------|------|------|-------|-------|------|--------------|
|               | ASME             | JIS         | C              | Cr    | Ni    | Co    | Si   | Al   | W    | Cu   | Mo   | Nb   | Mn   | V    | B     | N     | Ti   | Misc         |
| 18Cr-8Ni      | TP304H           | SUS304HTB   | 0.08           | 18.00 | 8.00  |       | 0.60 |      |      |      |      | 1.60 |      |      |       |       |      |              |
|               | Super304H        | SUS304J1HTB | 0.10           | 18.00 | 9.00  |       | 0.20 |      |      | 3.00 |      | 0.40 | 0.80 |      |       | 0.10  |      |              |
|               | TP321H           | SUS321HTB   | 0.08           | 18.00 | 10.00 |       | 0.60 |      |      |      |      |      | 0.80 |      |       |       |      | 0.50         |
|               | Tempaloy A-1     | SUS321J1HTB | 0.12           | 18.00 | 10.00 |       | 0.60 |      |      |      |      |      | 1.60 |      |       |       |      | 0.08         |
|               | TP316H           | SUS316HTB   | 0.08           | 16.00 | 12.00 |       | 0.60 |      |      |      | 2.50 |      | 1.60 |      |       |       |      |              |
|               | TP347H           | SUSTP347HTB | 0.08           | 18.00 | 10.00 |       | 0.60 |      |      |      |      |      | 0.80 | 1.60 |       |       |      |              |
| 15Cr-15Ni     | TP347HFG         |             | 0.08           | 18.00 | 10.00 |       | 0.60 |      |      |      |      | 0.80 | 1.60 |      |       |       |      |              |
|               | 17-14CuMo        |             | 0.12           | 16.00 | 14.00 |       | 0.50 |      |      | 3.00 | 2.00 | 0.40 | 0.70 |      | 0.006 |       | 0.30 |              |
|               | Esshete 1250     |             | 0.12           | 15.00 | 10.00 |       | 0.50 |      | 0.20 |      | 1.00 |      | 6.00 | 1.00 |       |       | 0.06 |              |
|               | Tempaloy A-2     |             | 0.12           | 18.00 | 14.00 |       | 0.60 |      |      |      | 1.60 | 0.24 | 1.60 |      |       |       | 0.10 |              |
| 20-25Cr       | TP310            | SUS310TB    | 0.08           | 25.00 | 20.00 |       | 0.60 |      |      |      |      |      | 1.60 |      |       |       |      |              |
|               | TP310NbN         | SUS310J1TB  | 0.06           | 25.00 | 20.00 |       | 0.40 |      |      |      |      |      | 0.45 | 1.20 |       | 0.20  |      | 0.045P 0.03S |
|               | TP310HCbN (HR3C) |             | 0.06           | 25.00 | 20.00 |       | 0.40 |      |      |      |      |      | 0.45 | 1.20 |       | 0.20  |      |              |
|               | NF707*           |             | 0.08           | 21.00 | 35.00 |       | 0.50 |      |      |      | 1.50 | 0.20 | 1.00 |      |       |       |      | 0.10         |
|               | Alloy 800H       | NCF800HTB   | 0.08           | 21.00 | 32.00 |       | 0.50 | 0.40 |      |      |      |      | 1.20 |      |       |       |      | 0.50         |
|               | Tempaloy A-3     | SUS309J4HTB | 0.05           | 22.00 | 15.00 |       | 0.40 |      |      |      |      |      | 0.70 | 1.50 |       | 0.002 | 0.15 |              |
| HighCr-HighNi | NF709*           | SUS310J2TB  | 0.15           | 20.00 | 25.00 |       | 0.50 |      |      |      | 1.50 | 0.20 | 1.00 |      |       |       | 0.10 |              |
|               | SAVE25*          |             | 0.10           | 23.00 | 18.00 |       | 0.40 |      | 1.50 | 3.00 |      | 0.45 | 1.00 |      |       | 0.20  |      |              |
|               | CR30A*           |             | 0.06           | 30.00 | 50.00 |       | 0.30 |      |      |      |      | 2.00 |      | 0.20 |       |       |      | 0.20         |
|               | HR6W*            |             | 0.08           | 23.00 | 43.00 |       | 0.40 |      |      | 6.00 |      |      | 0.18 | 1.20 |       | 0.00  |      | 0.08         |
|               | Inconel 617      |             |                | 22.00 | 54.00 | 12.50 | 0.40 | 1.20 |      |      |      | 8.50 |      | 0.40 |       |       |      |              |
|               | Inconel 671      |             | 0.05           | 48.00 | 51.50 |       |      |      |      |      |      |      |      |      |       |       |      |              |

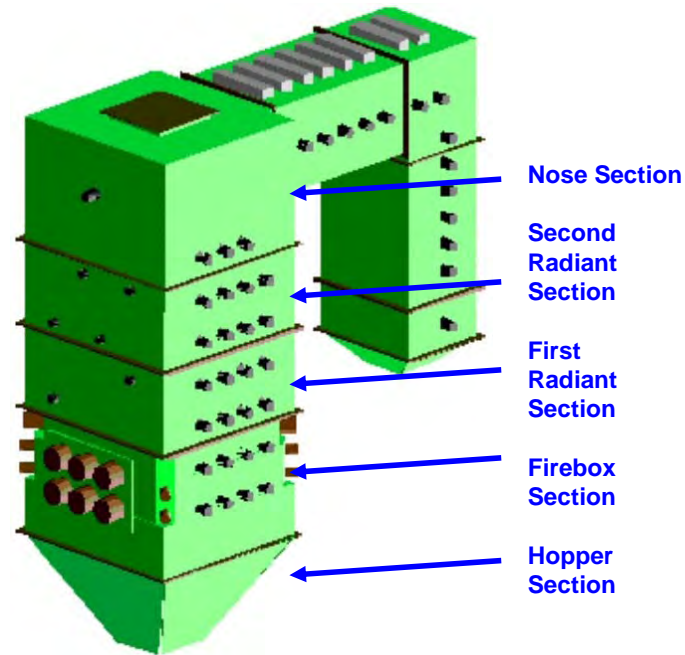
Argonne National Laboratory, 2002

# Candidate USC Material in Korea

→ Three ferrite and three austenite: T92, T91, T122, HR3C, S304H, and TP347HFG

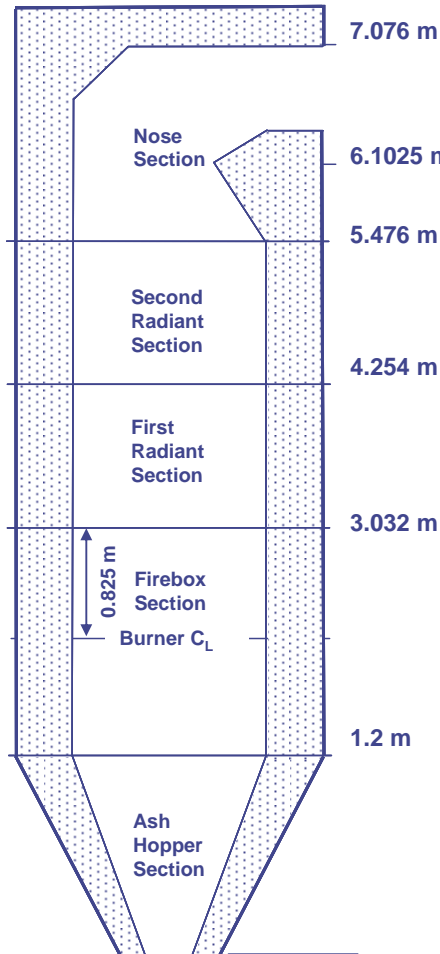
| Candidate | Composition, % |     |       |      |      |    |     |    |     |      |      |      |       |       | Comments  |
|-----------|----------------|-----|-------|------|------|----|-----|----|-----|------|------|------|-------|-------|-----------|
|           | C              | Fe  | Cr    | Ni   | Si   | Al | W   | Cu | Mo  | Nb   | Mn   | V    | B     | N     |           |
| T92       | 0.07           | Bal | 9     | -    | 0.06 | -  | 1.8 |    | 0.5 | 0.05 | 0.45 | 0.2  | 0.004 | 0.06  | Ferrite   |
| T122      | 0.1            | Bal | 11    | -    | 0.1  | -  | 2   | 1  | 0,4 | 0,05 | 0.6  | 0,20 | 0.003 | 0.06  | Ferrite   |
| HR3C      | 0.06           | Bal | 25    | 20   | 0.4  | -  | -   |    | -   | 0.45 | 1.2  | -    | -     | 0.2   | Austenite |
| T91       |                | Bal | 9     |      |      |    |     |    | 1   |      |      |      |       |       | Ferrite   |
| S304H     | 0.1            | Bal | 18.15 | 9.25 | 0.27 |    |     | 3  |     | 0.4  | 0.78 |      |       | 0.091 | Austenite |
| TP347HFG  | 0.08           | Bal | 18    | 10   | 0.6  |    |     |    |     | 0.8  | 1.6  |      |       |       | Austenite |

# KEPRI Pilot-scale Test Furnace



- ➔ 5 MMBtu/hr on natural gas or coal
- ➔ Convertible firing methods: corner or wall-fired
- ➔ Furnace inside dimension: 1.6 x 1.9 x 7.1 meters (depth x width x height)
- ➔ Refractory casting

# Refractory and Cooling Tubes



## Nose Section Roof

- Castable: CT-155S, 10", k = 0.6978 W/m/°C
- Insulation: HTB, 2", k = 0.11 W/m/°C
- Carbon Steel, 0.38", k = 60 W/m/°C
- Total thermal resistance = 0.550 m<sup>2</sup>°C/W

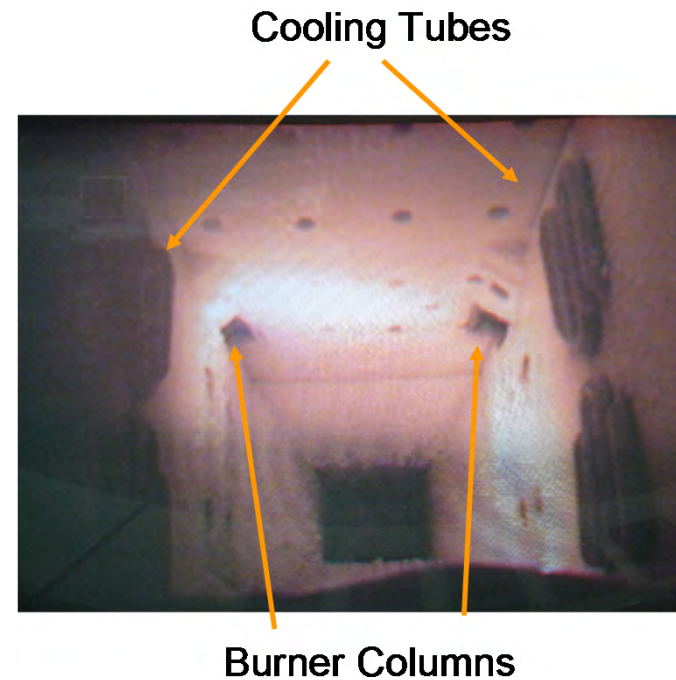
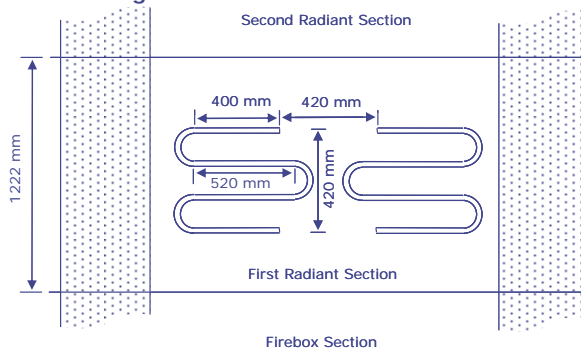
## Radiant Sections 1 & 2, Nose Section Walls

- Castable: CT-155S, 14", k = 0.6978 W/m/°C
- Insulation: HTB, 4", k = 0.11 W/m/°C
- Carbon Steel, 0.38", k = 60 W/m/°C
- Total thermal resistance = 1.448 m<sup>2</sup>°C/W

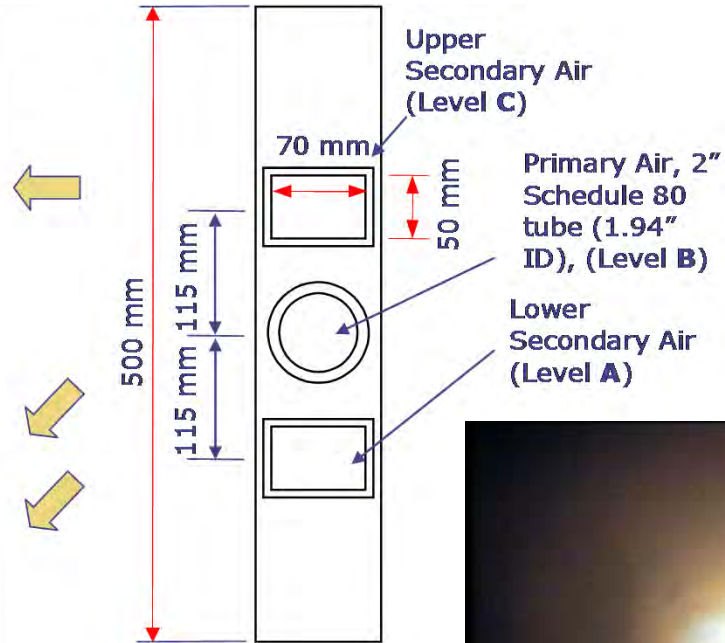
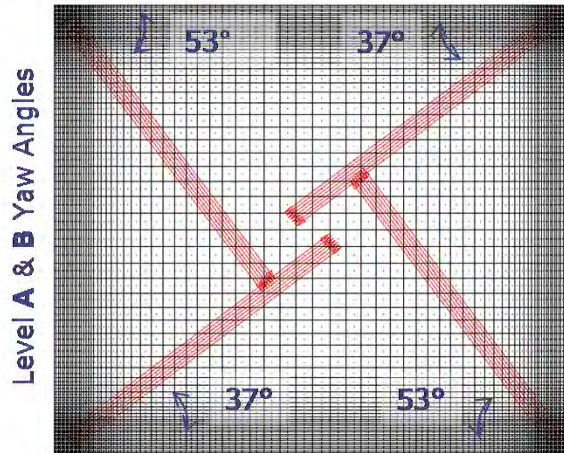
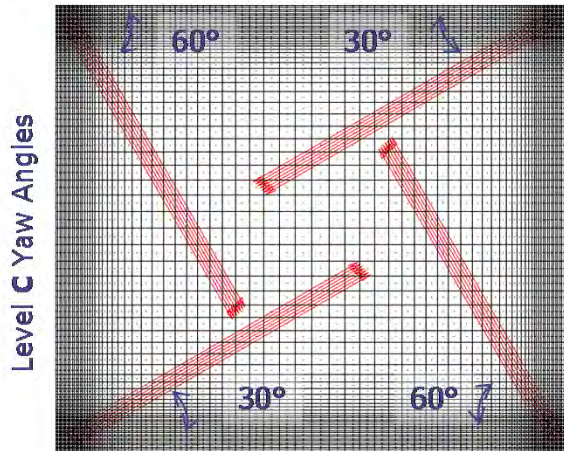
## Ash Hopper & Burner Region

- Fire Brick: AI 85C, 4.5", k = 2.89 W/m/°C
- Castable: INCT-165S, 9.5", k = 0.5465 W/m/°C
- Insulation: Cerakwool, 4", k = 0.13 W/m/°C
- Carbon Steel, 0.38", k = 60 W/m/°C
- Total thermal resistance = 1.263 m<sup>2</sup>°C/W

## Cooling Tubes



# Burner Arrangement



Mirror Image

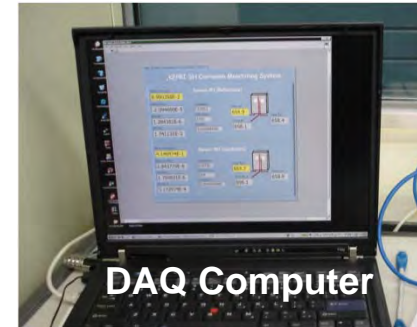
# Corrosion Monitoring System



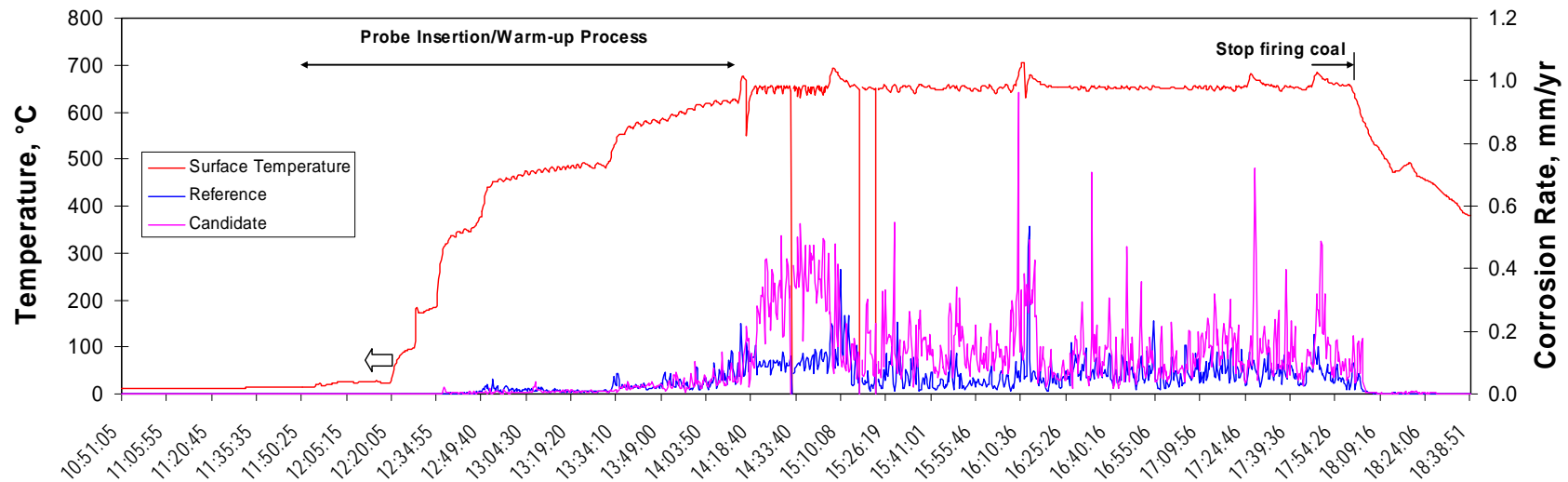
Installed Probe



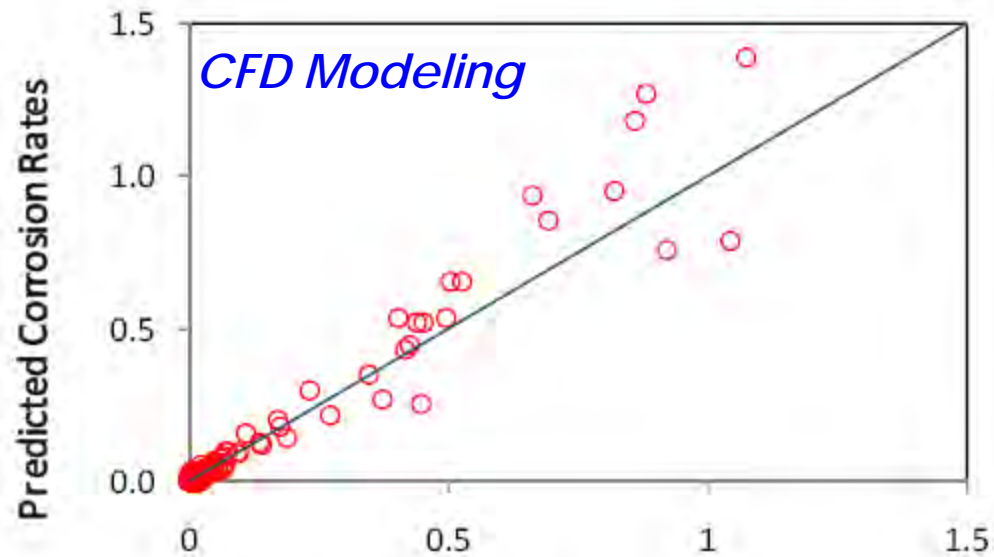
Control Box



DAQ Computer

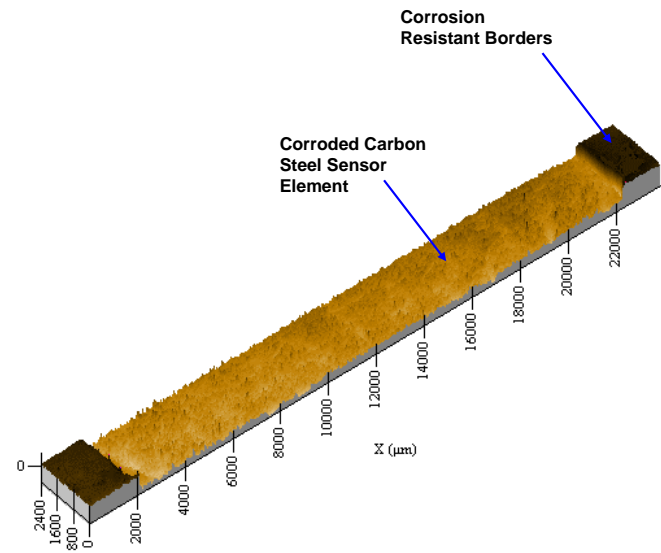
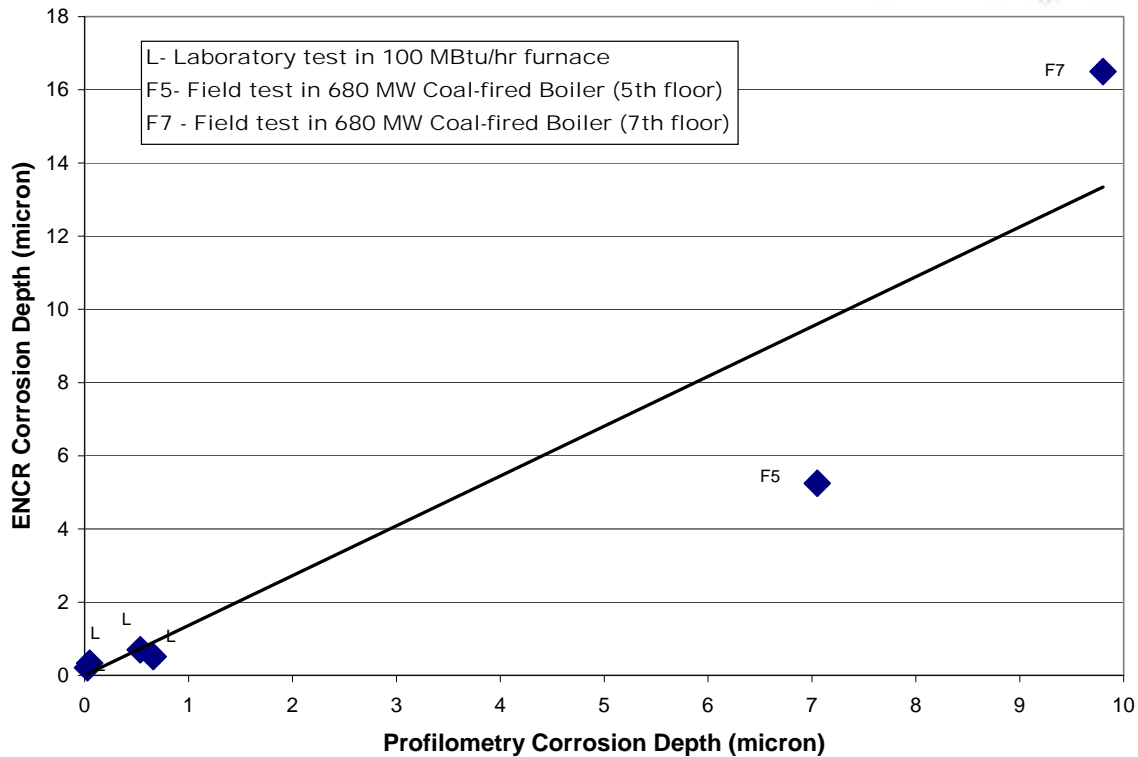


# Quantitative Validation

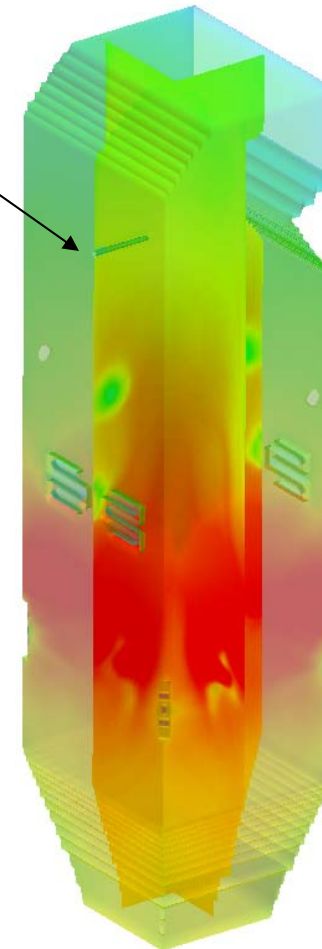
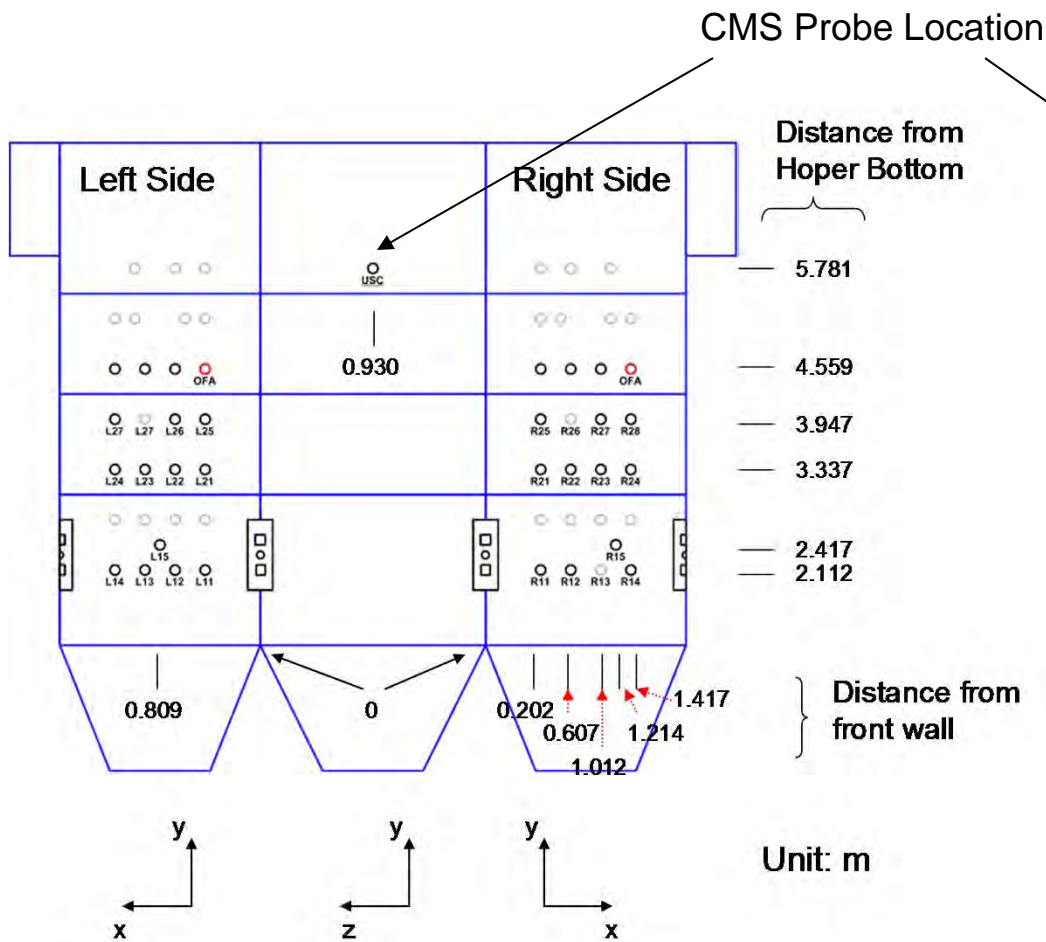


Measured Corrosion Rates

## Profilometry



# Probe Location



# Operating Conditions

|                                   | Unit       | OP1   |
|-----------------------------------|------------|-------|
| <b>Coal</b>                       |            | C&A   |
| Coal Feeding Rate                 | kg/hr      | 180   |
| Firing Rate                       | MW         | 1.45  |
| <b>Particle Size Distribution</b> | % 200 mesh | 70    |
| <b>Excess O<sub>2</sub></b>       | wet%       | 3.6   |
| <b>Burner Stoichiometry</b>       |            | 0.9   |
| <b>Excess Air</b>                 | %          | 20    |
| <b>Primary Air/Fuel</b>           |            | 1.9   |
| <b>Combustion Air</b>             |            |       |
| Primary                           | kg/s       | 0.095 |
| Secondary                         | kg/s       | 0.472 |
| Burner Secondary                  |            | 0.330 |
| <i>Burner Sec A (bottom)</i>      | kg/s       | 0.165 |
| <i>Burner Sec C (top)</i>         | kg/s       | 0.165 |
| Overfire Air                      | kg/s       | 0.142 |
| Total Combustion Air              | kg/s       | 0.567 |
| Air Temperature                   |            |       |
| Primary                           | °C         | 58    |
| Secondary                         | °C         | 272   |

- ➔ C&A coal is used.
- ➔ Excess air: 20%
- ➔ Burner Stoichiometry: 0.9
- ➔ Primary Air/Fuel : 1.9
- ➔ Firing Rate: 1.45MWth
- ➔ Corrosion rates were measured at the metal temperatures of 650, 675, and 700°C.

# C&A Coal Properties

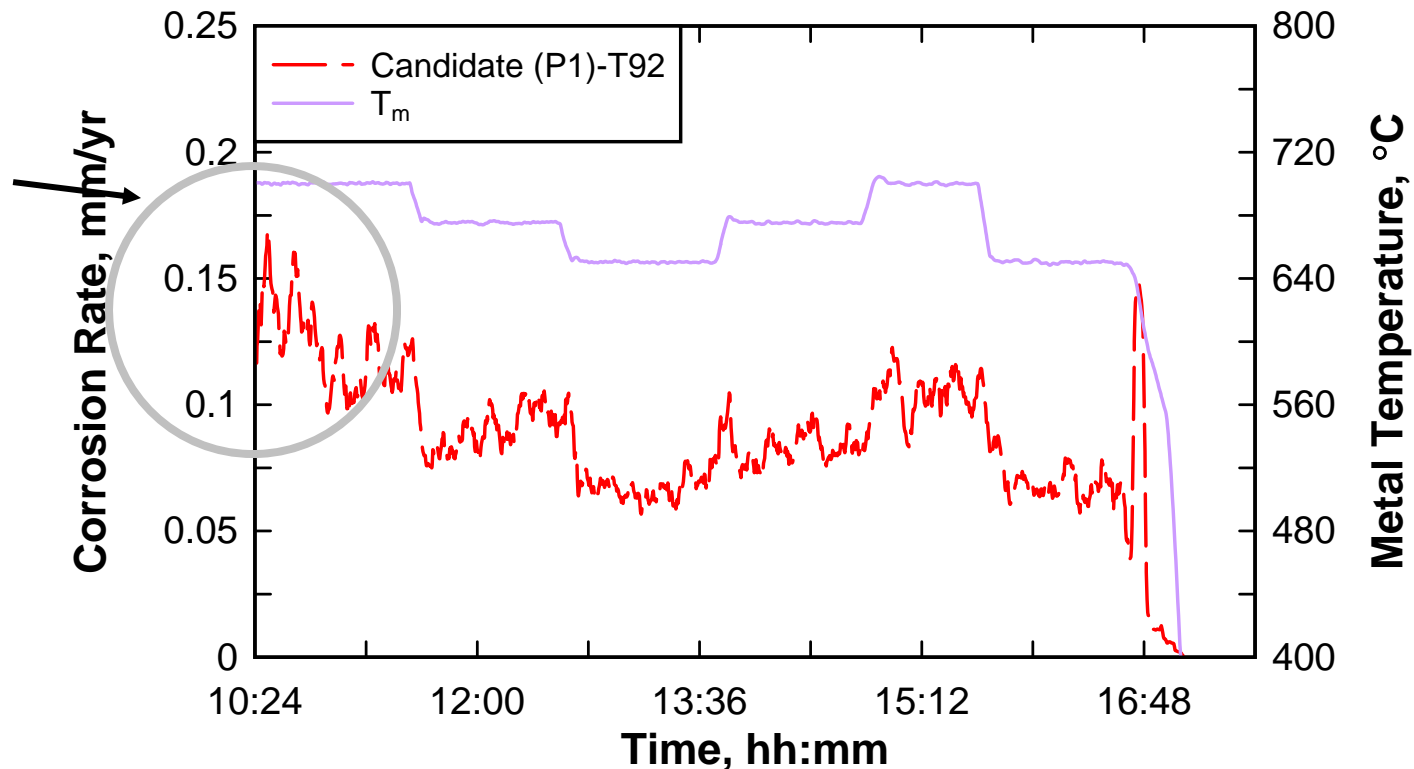
| Ultimate Analysis  |        |
|--------------------|--------|
| Composition (wt%)  | C&A    |
| C                  | 69.62  |
| H                  | 4.80   |
| O                  | 5.66   |
| N                  | 1.52   |
| S                  | 0.61   |
| ash                | 13.44  |
| H <sub>2</sub> O   | 4.34   |
| Total              | 100.00 |
| Proximate Analysis |        |
|                    | C&A    |
| Fixed Carbon       | 53.00  |
| Volatile           | 29.22  |
| Ash                | 13.44  |
| Moisture           | 4.34   |
| Total              | 100.00 |
| Heating Value      |        |
|                    | C&A    |
| LHV, kcal/kg       | 6618   |
| HHV, kcal/kg       | 6930   |

|  |                                | C&A   |
|--|--------------------------------|-------|
| A<br>S<br>H<br><br>(<br>w<br>t<br>%<br>) | SiO <sub>2</sub>               | 70.14 |
|  | Al <sub>2</sub> O <sub>3</sub> | 19.25 |
|  | Fe <sub>2</sub> O <sub>3</sub> | 3.6   |
|  | CaO                            | 1.4   |
|  | MgO                            | 0.8   |
|  | Na <sub>2</sub> O              | 0.54  |
|  | K <sub>2</sub> O               | 0.96  |
|  | TiO <sub>2</sub>               | 0.84  |
|  | SO <sub>3</sub>                | 0.8   |

- Low sulfur (0.61 wt%) and chlorine (0.035 wt%)
- Fuel corrosivity ~ 0.11 based on Na, K, Ca, Mg, S contents

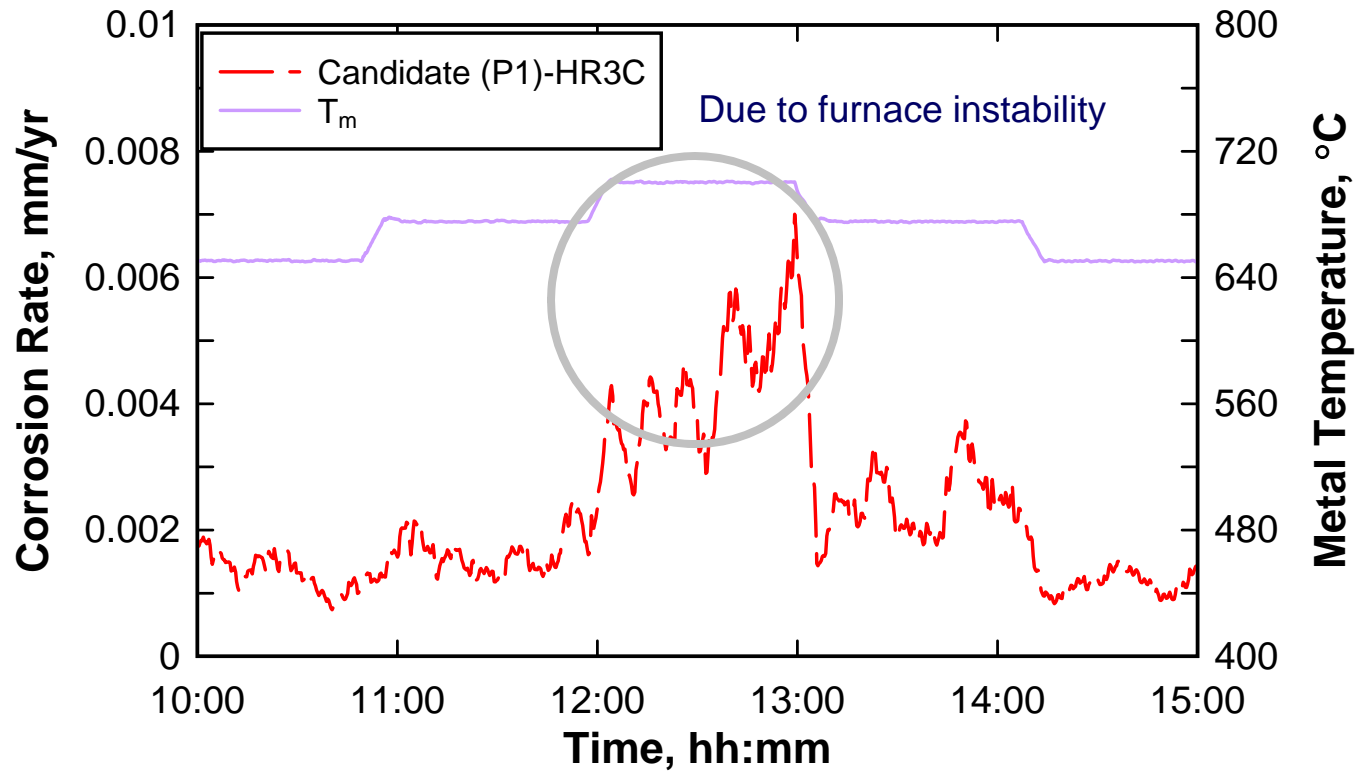
# Corrosion Rate – T92

Initial conditioning of the metal



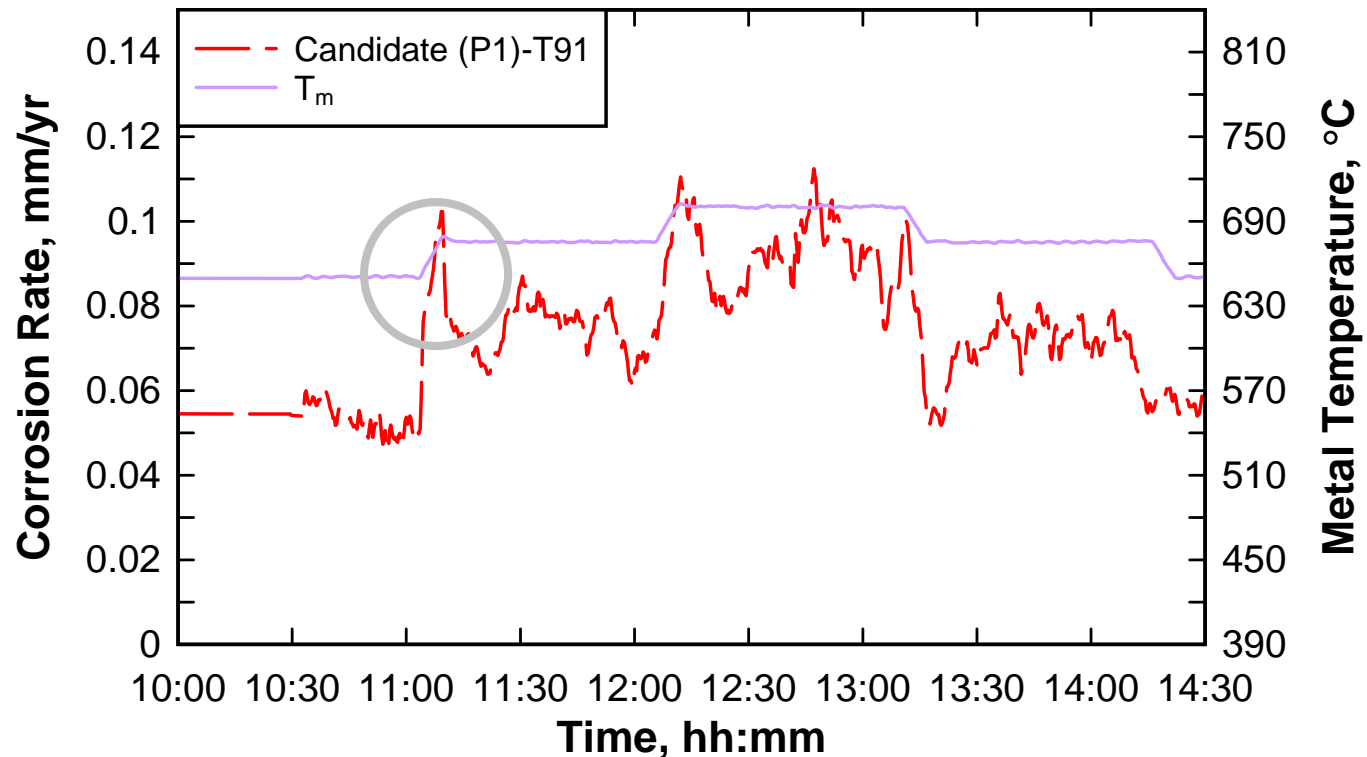
→ Corrosion rates varied according to the metal temperature change.

# Corrosion Rates – HR3C



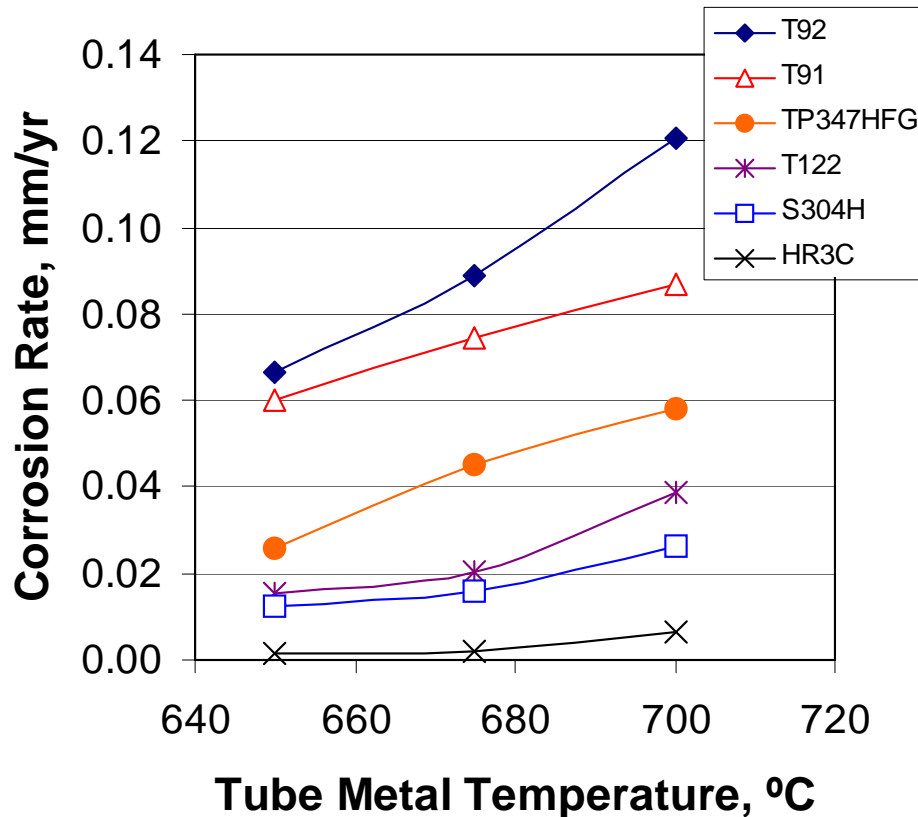
➔ Low corrosion rates at all temperatures

# Corrosion Rates - T91



- ➔ Corrosion rates varied according to the metal temperature change.
- ➔ Relatively high corrosion rates when the temperature changed.
- ➔ Similar corrosion rates to that of T92

# Material Comparison



## → Corrosion Rates:

T92 > T91 > TP347HFG > T122  
> S304H > HR3C

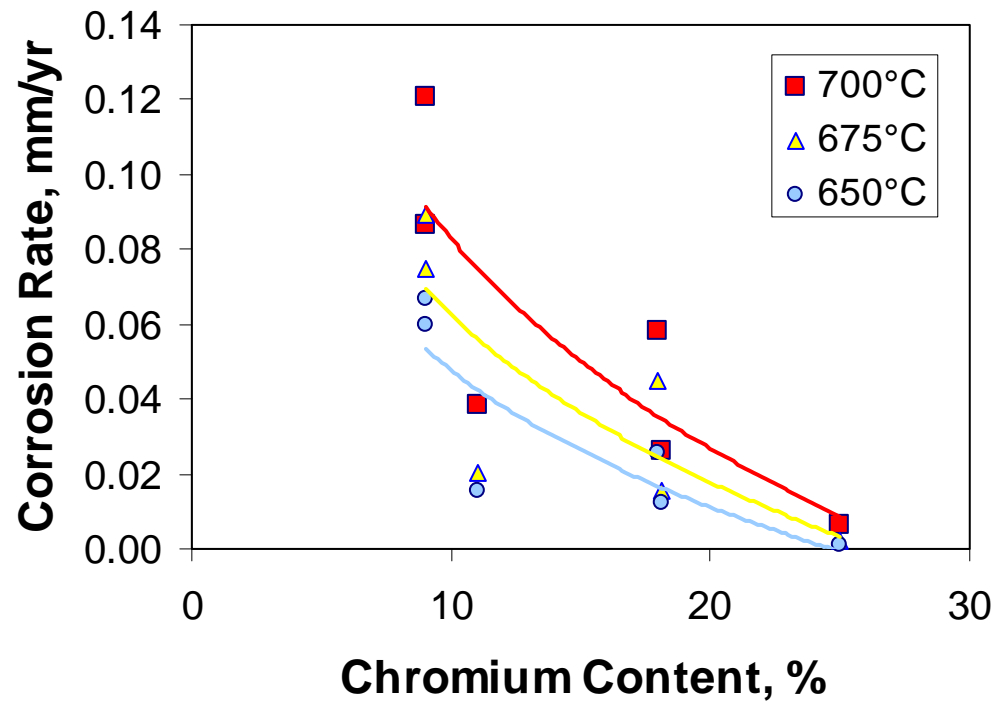
→ Corrosion rates increased with increasing metal temperature

→ The difference between the materials becomes larger with increasing temperature in some cases.

# Corrosion Rates vs. Cr Contents

---

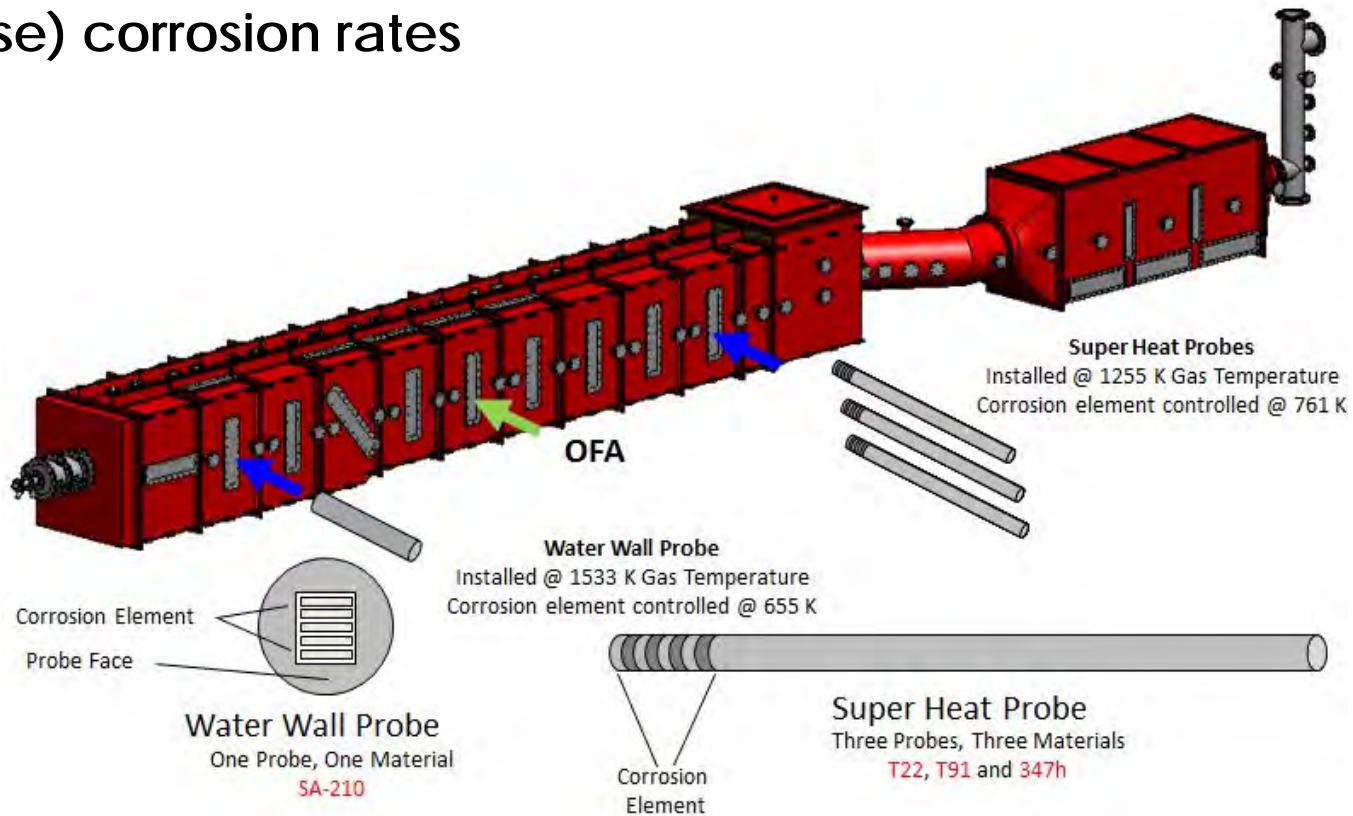
---



- ➔ Corrosion rates increased with decreasing chromium contents.
- ➔ TP347HFG and T122 show exception.

# Corrosion under Oxy-coal Firing

Oxy-combustion under possible retrofit conditions affects both waterwall (slight decrease) and superheat (significant increase) corrosion rates



# Corrosion Element Material Analysis

| Material   | SA 210    | T22       | P91       | 347H      |
|------------|-----------|-----------|-----------|-----------|
| HT Surface | Waterwall | Superheat | Superheat | Superheat |
| C          | 0.07      | 0.11      | 0.10      | 0.048     |
| Si         | 0.23      | 0.2       | 0.32      | 0.40      |
| Mn         | 0.42      | 0.44      | 0.47      | 1.32      |
| Ni         | -         | -         | 0.15      | 9.73      |
| Cr         | -         | 2.21      | 8.52      | 17.45     |
| Mo         | -         | 0.95      | 0.93      | -         |
| S          | 0.002     | 0.003     | 0.002     | 0.008     |
| P          | 0.009     | 0.01      | 0.018     | 0.026     |
| Cu         | -         | -         | 0.11      | -         |
| Al         | -         | -         | 0.01      | 0.005     |
| Nb/Cb      | -         | -         | 0.07      | 0.63      |
| V          | -         | -         | 0.22      | 0.078     |
| N          | -         | -         | 0.044     | -         |
| Ta         | -         | -         | -         | 0.02      |

\* All values in mass %

# Normal Operating Conditions



Superheat corrosion probe (347h)

## → Probe Element Temperatures

- ◆ SA210 (655– 728 K)
- ◆ T22 (761 – 839 K)
- ◆ P91 (761 - 866 K)
- ◆ 347h (761 – 978 K)

## → Gas Temperatures

- ◆ Water wall probe ~ 1533 K
- ◆ Superheat probes ~ 1255 K

## → SO<sub>2</sub> Concentrations

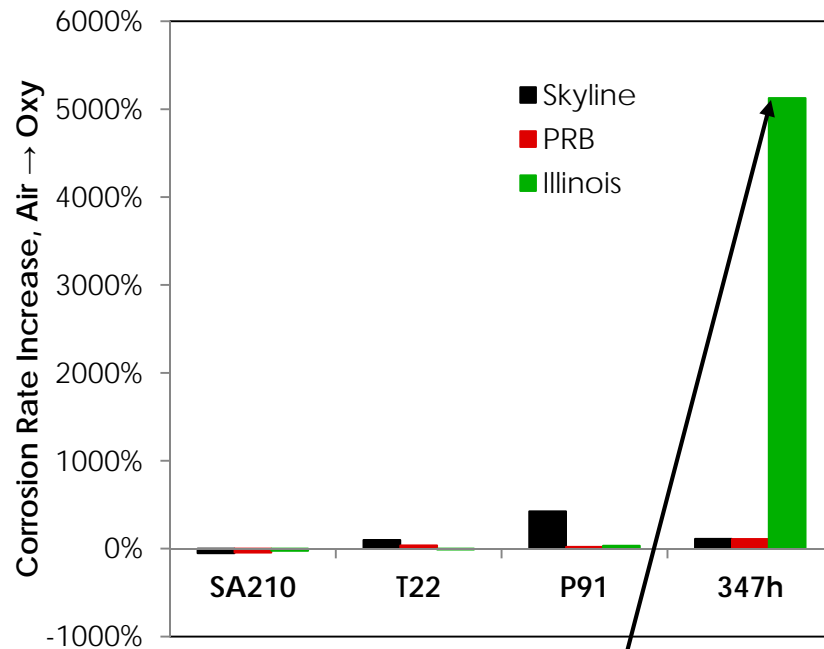
- ◆ Utah, Air ~ 500 ppmv
- ◆ Utah, Oxy ~ 1,800 ppmv
- ◆ PRB, Air ~ 100 ppmv
- ◆ PRB, Oxy ~ 300 ppmv
- ◆ Illinois, Air ~ 3,000 ppmv
- ◆ Illinois, Oxy ~ 18,000 ppmv

## → Oxidizing / Reducing Conditions

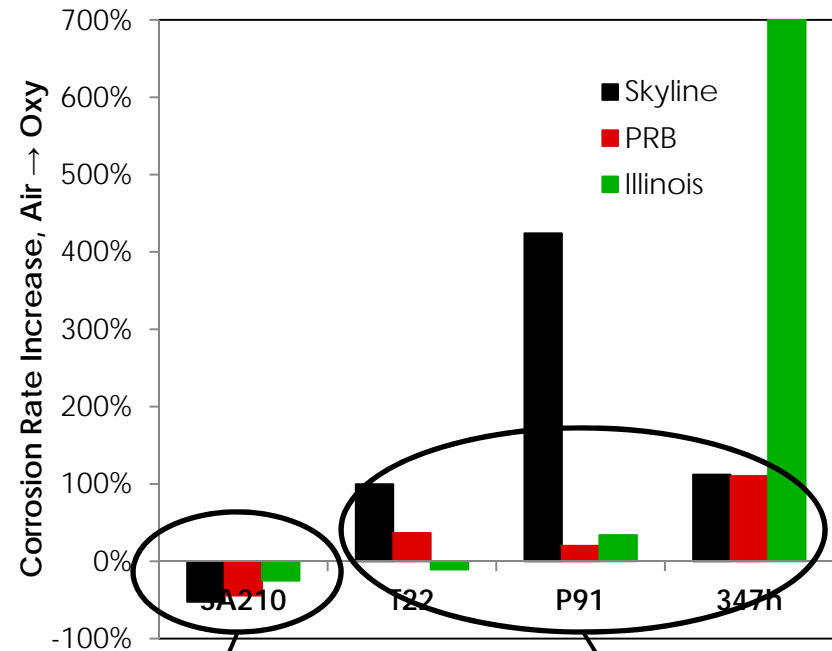
- ◆ Water wall probe – Mostly reducing conditions (BSR = 0.9)
- ◆ Superheat probes – Oxidizing conditions

# Increase in Corrosion Rate Air → Oxy

Baseline sensor element temperatures, probe locations and staging conditions



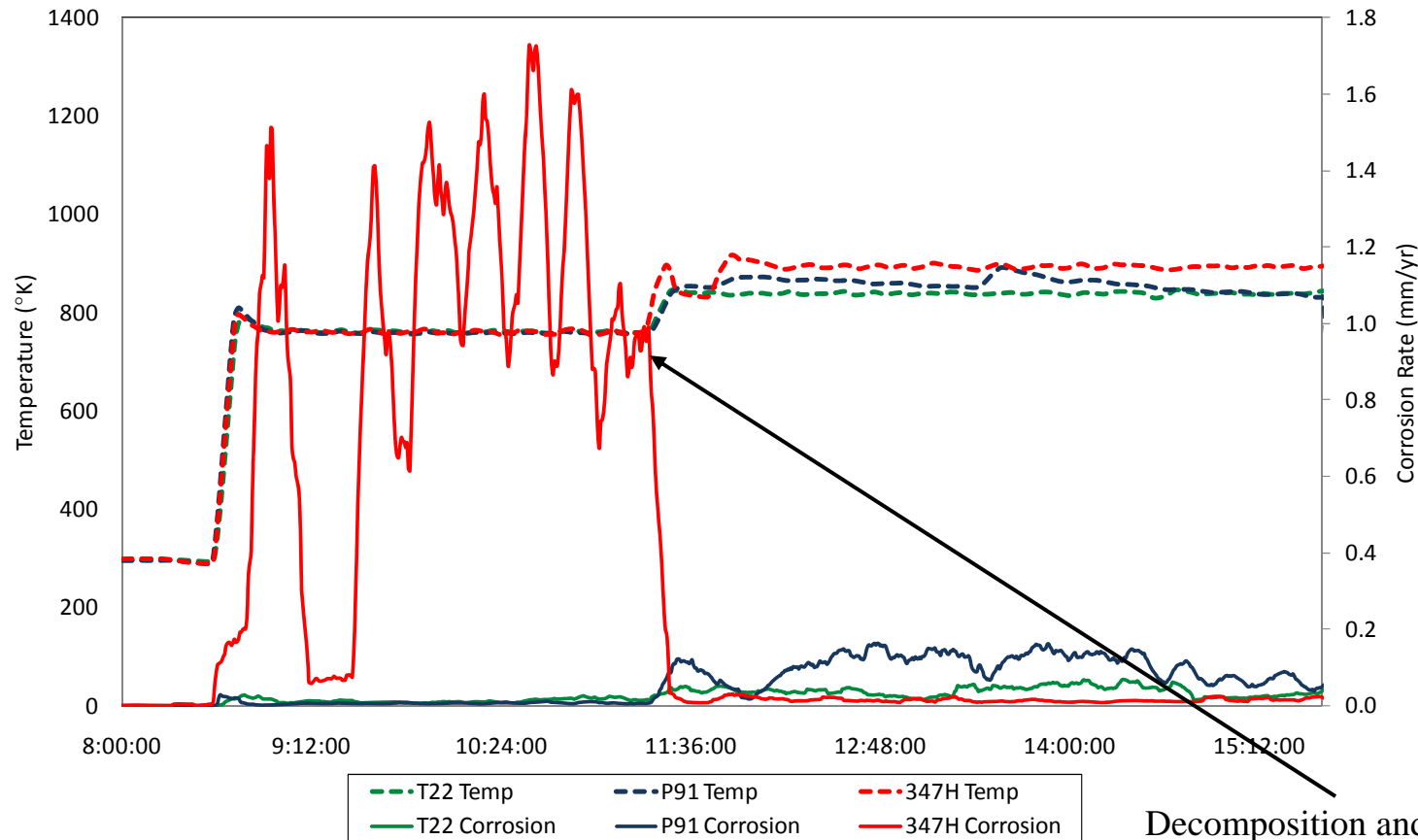
Wow, Why?



Waterwall Probe  
↓ Corrosion  
Air → Oxy Combustion

Superheat Probes  
Generally ↑ Corrosion  
Air → Oxy Combustion

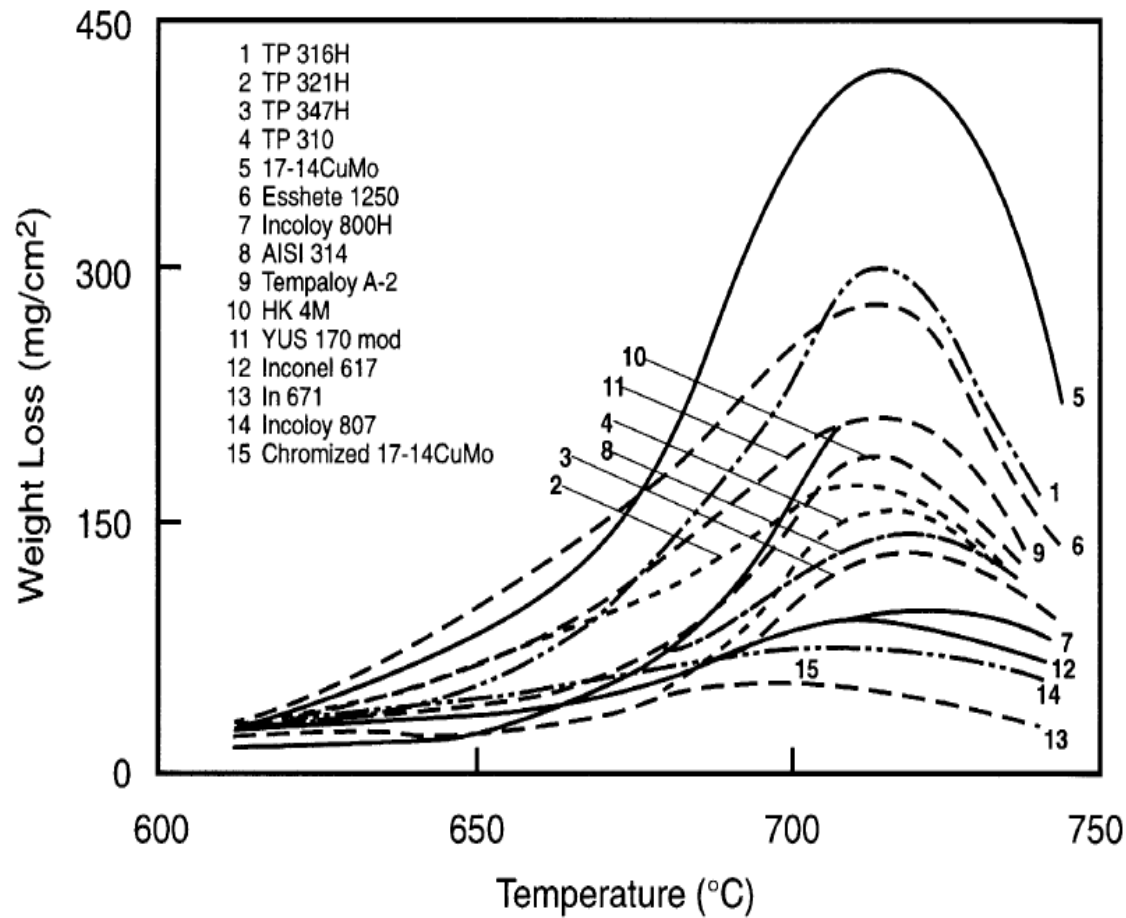
# Temperature Effects on Corrosion



Decomposition and volatilization of the trisulphate species  
(Viswanathan and Bakker, 2000)

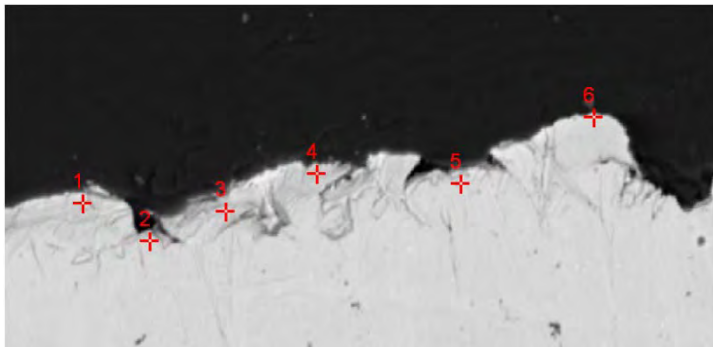
Operation of 347H at subcritical temperatures in the presence of high SO<sub>2</sub> concentrations will produce extremely high corrosion rates.

# Alkali Iron Trisulfate Decomposition

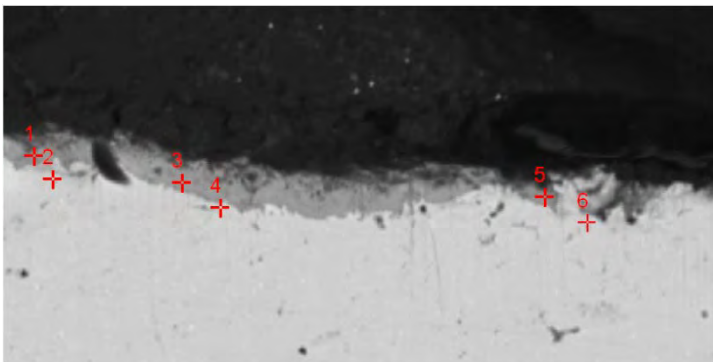


# 347H Metallographic Results

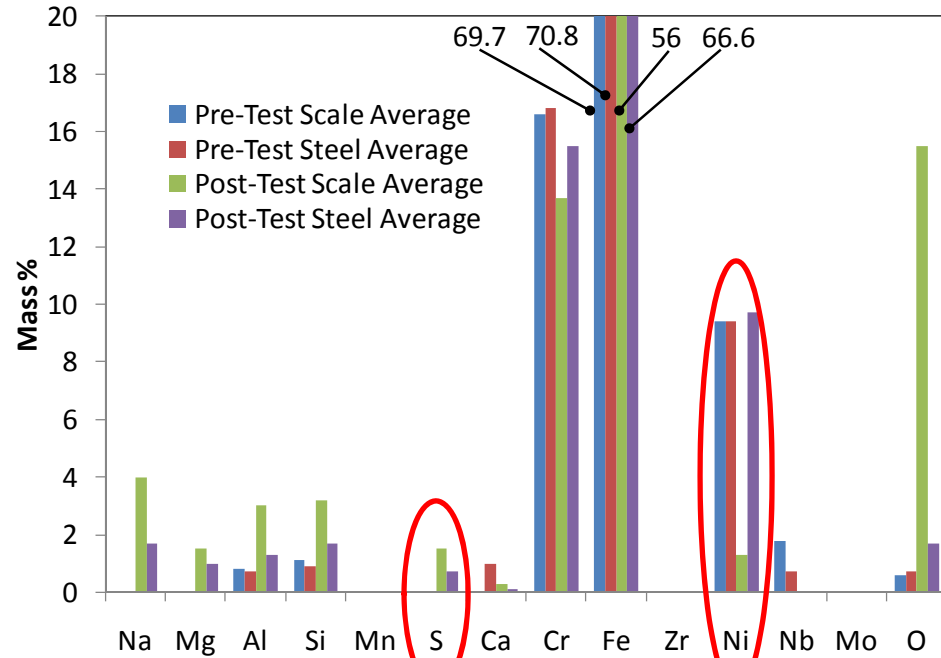
Backscattered Electron Images of the 347H Corrosion Element



Pre-Combustion Testing



Post-Combustion Testing



Sulfur is present in the post-test scale and steel

Nickel has been removed in the post-test scale

---

---

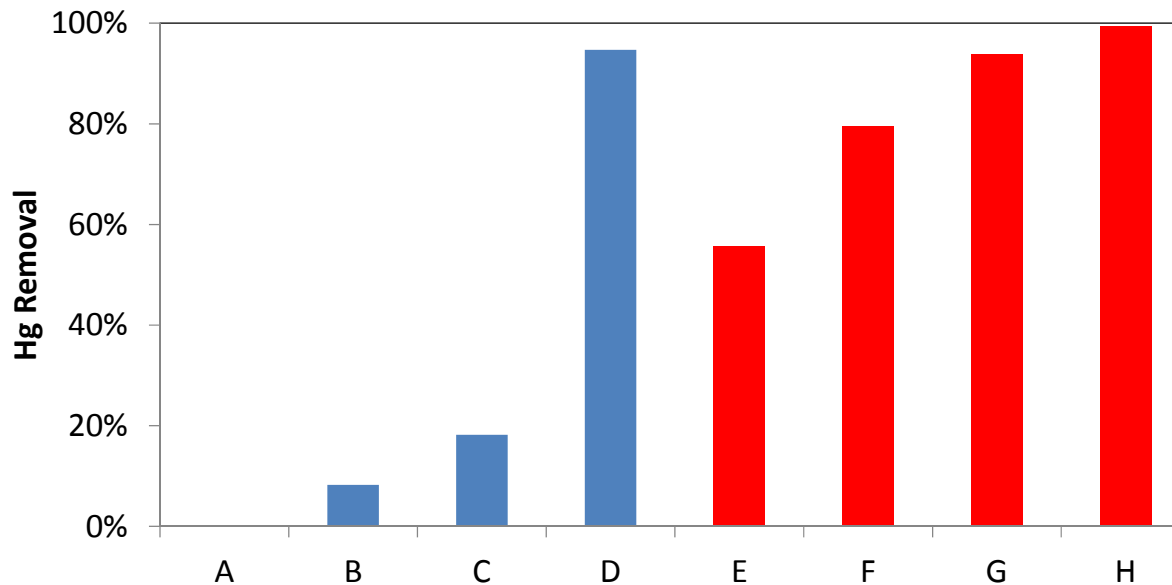
# Air Heater Corrosion

---

---

# Evaluation of Hg Control Options

MerSim™ total plant simulation



| Case | Description         | Plant Configuration             | ACI                    | Boiler Additive | Hg removal |
|------|---------------------|---------------------------------|------------------------|-----------------|------------|
| A    | Baseline            | Boiler + APH + ESP              |                        |                 | 0.0%       |
| B    | Co-benefit          | Boiler + SCR + APH + ESP + wFGD |                        |                 | 8.2%       |
| C    | Additive            | Boiler + APH + ESP              |                        | 3 gal/hr KNX    | 18.2%      |
| D    | Additive-Co-benefit | Boiler + SCR + APH + ESP + wFGD |                        | 3 gal/hr KNX    | 94.7%      |
| E    | ACI-ESP             | Boiler + APH + ESP              | 2 lb/MMacf Darco Hg    |                 | 55.6%      |
| F    | ACI-FF              | Boiler + APH + FF               | 2 lb/MMacf Darco Hg    |                 | 79.6%      |
| G    | BrACI-FF            | Boiler + APH + FF               | 2 lb/MMacf Darco Hg-LH |                 | 93.9%      |
| H    | Additive-ACI-ESP    | Boiler + APH + ESP              | 2 lb/MMacf Darco Hg    | 3 gal/hr KNX    | 99.3%      |

# Bromine and APH Corrosion

---

---

- ➔ Brominated activated carbon injection (Br-ACI) can accelerate APH corrosion rates
  - ◆ Supplier-dependent impacts have been noted
  - ◆ Low temps in APH suspected to exacerbate problem
- ➔ EPRI/URS boiler bromide addition study [Dombrowski, 2013]
  - ◆ 52 units with > 1yr operation had conducted inspections
  - ◆ 24 of these units noted accelerated corrosion
  - ◆ Increased corrosion in PRB/lignite units has been particularly severe

# Possible APH Corrosion Mechanisms

---

---

## → Possible Mechanisms:

- ◆ Direct condensation of HBr
- ◆ Absorption of HBr by condensed  $\text{SO}_3$
- ◆ Formation of Brominated salts on fly ash
- ◆ Gas-phase attack by HBr (higher Temp)

## → Condensation appears likely in this study

- ◆ Hydrobromic acid is one of the strongest mineral acids known
- ◆ Simple calculations for relevant concentrations of bromine addition indicate dew points in the 90-130 °F range
  - » 90-150 °F for this study
- ◆ Dew points for oxy-combustion as high as 150 °F

# Pilot-scale Corrosion Measurements

---

---

## Objective:

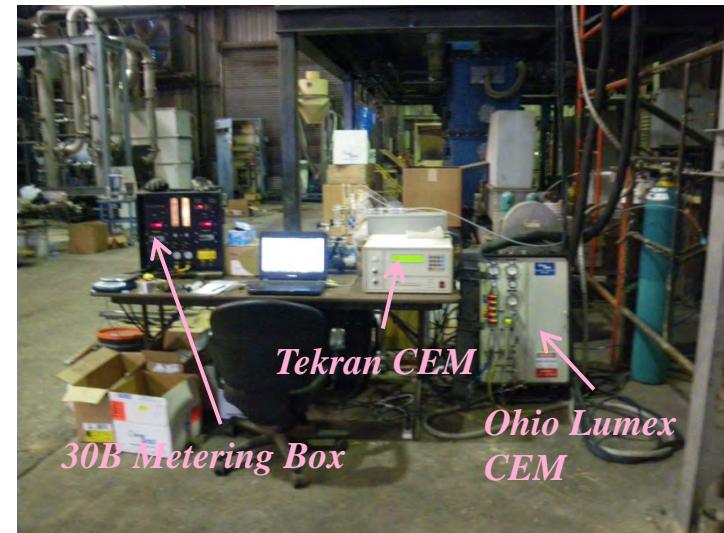
- Measure changes in corrosion rates at temperatures representative of an air heater,
- In the presence of various mercury control additives (baseline, bromine, activated carbon),
- Under both air-fired and oxy-fired conditions

## Method:

- Use air cooled corrosion probes positioned in the flue gas just upstream of the baghouse
- Vary probe cooling to control element surface temperature in a range considered representative of air heater temperatures, especially the colder extremes

# Complementary Pilot-Scale Measurements

- ➔ Objective - Measure impact of oxy-combustion on performance of mercury control technologies
- ➔ Approach
  - ◆ L1500 pilot-scale furnace
  - ◆ PRB and bituminous coals
  - ◆ Air and oxy-firing
  - ◆ Two Hg control technologies
    - » Bromine boiler additive ( $\text{CaBr}_2$ )
    - » Activated carbon injection
  - ◆ Hg measured before and after baghouse
  - ◆ Three different Hg measurement techniques
  - ◆ Testing in May and June 2013



# Operating Conditions

| Coal       | Condition | Firing Rate (kW) | O <sub>2</sub> (% dry) | CO <sub>2</sub> (% dry) | BH inlet (F) | BH outlet (F) |
|------------|-----------|------------------|------------------------|-------------------------|--------------|---------------|
| PRB        | Air-Fired | 780-860          | 4.0                    | 14                      | 380          | 250           |
| PRB        | Oxy-Fired | 780              | 3.5                    | 83                      | 300          | 140           |
| Bituminous | Air-Fired | 775-1025         | 3.5                    | 15                      | 356          | 239           |
| Bituminous | Oxy-Fired | 775-880          | 3.4                    | 87                      | 341          | 146           |




## Br addition:

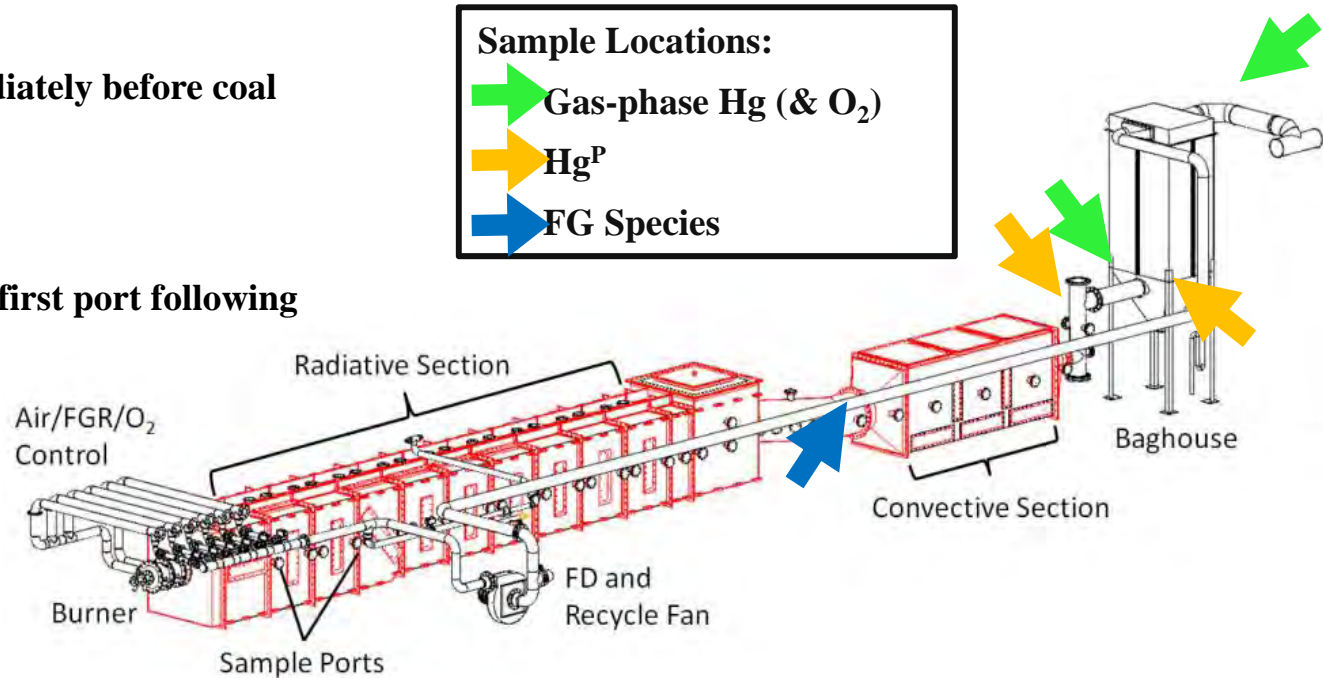
Solid CaBr<sub>2</sub> injected immediately before coal entered burner  
 (~8-75 ppm Br wet on coal)

## ACI:

Darco Hg injected through first port following convective section  
 (~0.5-10 lb/MMacf)

### Sample Locations:

-  Gas-phase Hg (& O<sub>2</sub>)
-  Hg<sup>P</sup>
-  FG Species

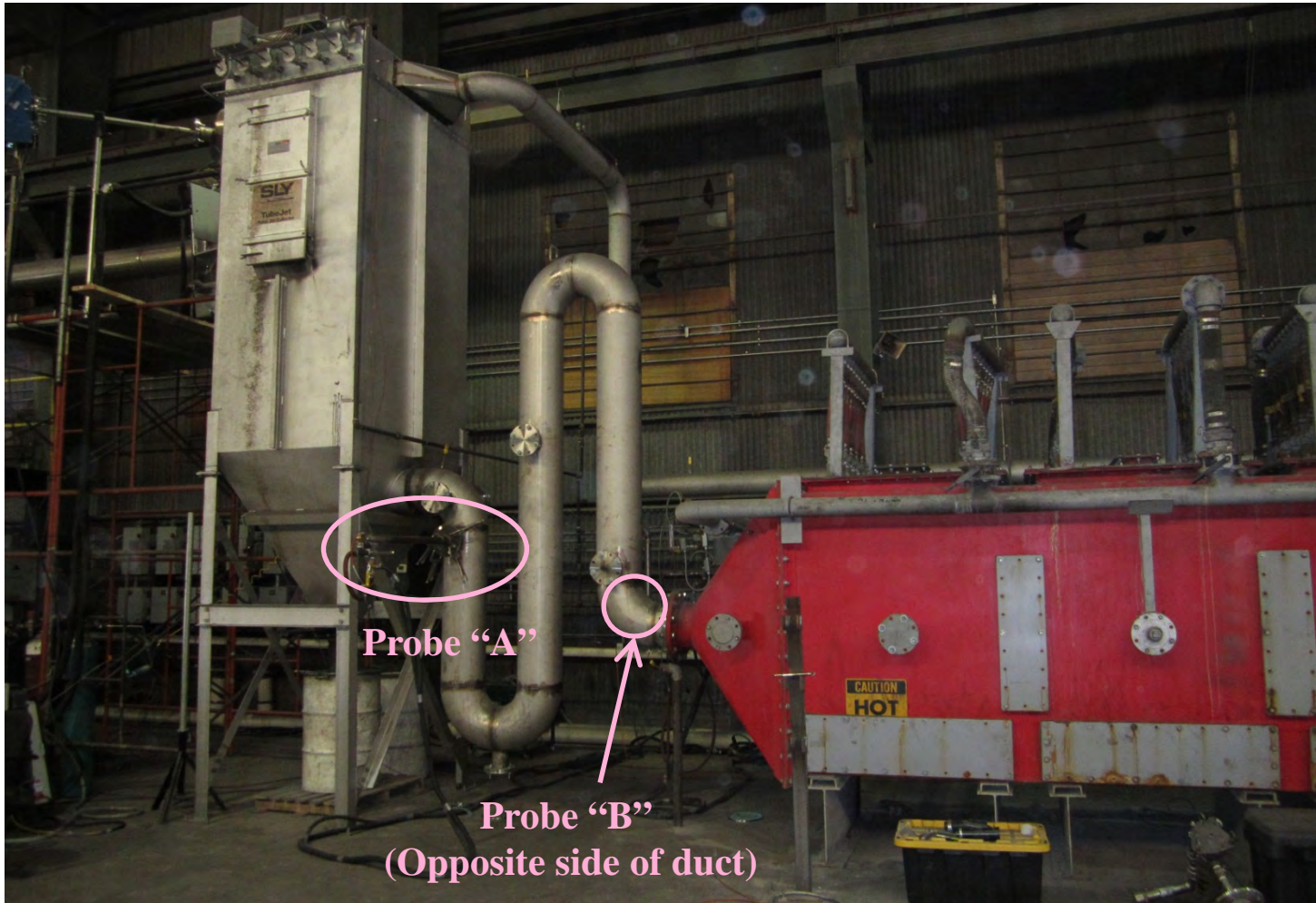


# Coal Analysis

| Black Thunder PRB      |             |                         |       |
|------------------------|-------------|-------------------------|-------|
| Coal Analyses          |             | Mineral Matter Analyses |       |
| <b>C</b>               | 54.04       | <b>Al</b>               | 14.19 |
| <b>H</b>               | 3.74        | <b>Ca</b>               | 16.13 |
| <b>N</b>               | 0.82        | <b>Fe</b>               | 5.99  |
| <b>S</b>               | 0.38        | <b>Mg</b>               | 3.33  |
| <b>O</b>               | 13.69       | <b>Mn</b>               | 0.04  |
| <b>Ash</b>             | 5.66        | <b>P</b>                | 0.71  |
| <b>Moisture</b>        | 21.67       | <b>K</b>                | 0.47  |
| <b>Volatile Matter</b> | 36.77       | <b>Si</b>               | 36.76 |
| <b>Fixed Carbon</b>    | 35.91       | <b>Na</b>               | 0.93  |
| <b>HHV, Btu/lb</b>     | 9320        | <b>S</b>                | 10.11 |
| <b>Hg, µg/g</b>        | 0.047±0.004 | <b>Ti</b>               | 1.11  |

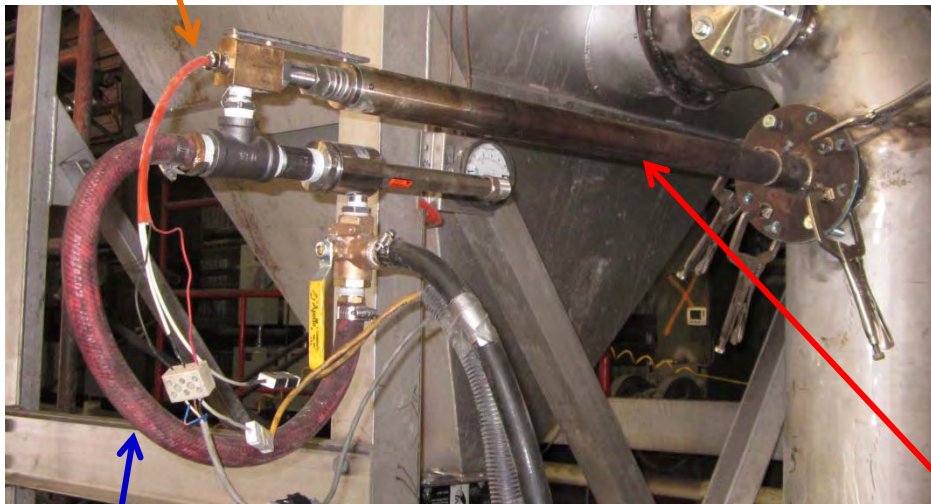
| Pratt Bituminous       |           |                         |       |
|------------------------|-----------|-------------------------|-------|
| Coal Analyses          |           | Mineral Matter Analyses |       |
| <b>C</b>               | 69.23     | <b>Al</b>               | 25.91 |
| <b>H</b>               | 4.82      | <b>Ca</b>               | 3.41  |
| <b>N</b>               | 1.69      | <b>Fe</b>               | 13.20 |
| <b>S</b>               | 2.22      | <b>Mg</b>               | 1.18  |
| <b>O</b>               | 6.54      | <b>Mn</b>               | 0.04  |
| <b>Ash</b>             | 13.14     | <b>P</b>                | 0.83  |
| <b>Moisture</b>        | 2.38      | <b>K</b>                | 2.33  |
| <b>Volatile Matter</b> | 35.64     | <b>Si</b>               | 44.78 |
| <b>Fixed Carbon</b>    | 48.85     | <b>Na</b>               | 0.47  |
| <b>HHV, Btu/lb</b>     | 12659     | <b>S</b>                | 3.72  |
| <b>Hg, µg/g</b>        | 0.21±0.01 | <b>Ti</b>               | 1.25  |

# Corrosion Probe Placement

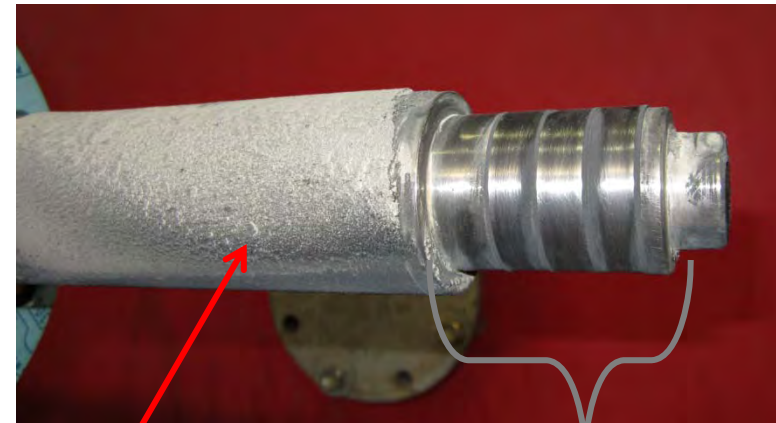


# ECN Corrosion Probes

Signal wires and  
thermocouple leads



Cooling air  
into probe

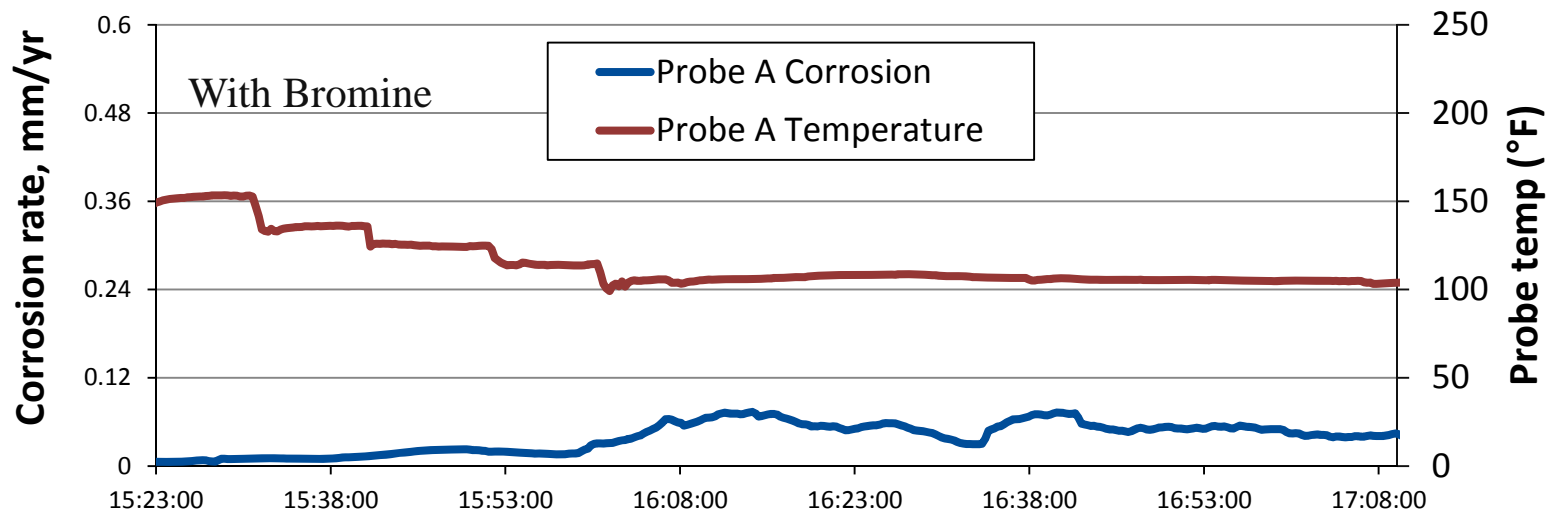
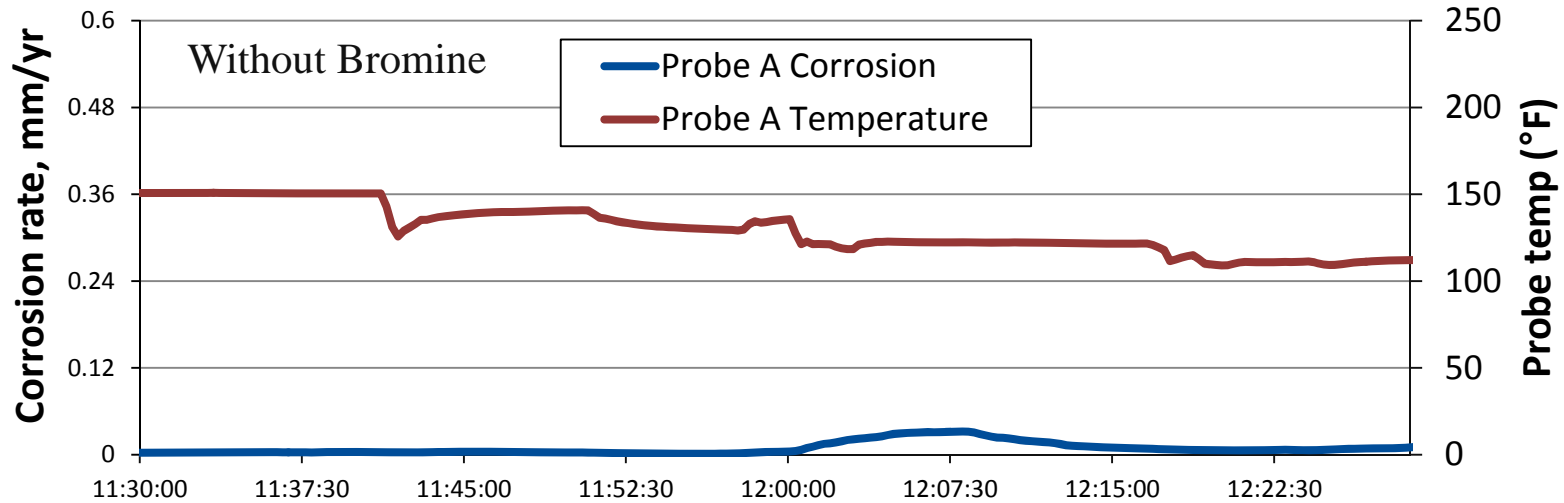


Stainless Steel  
Probe Body

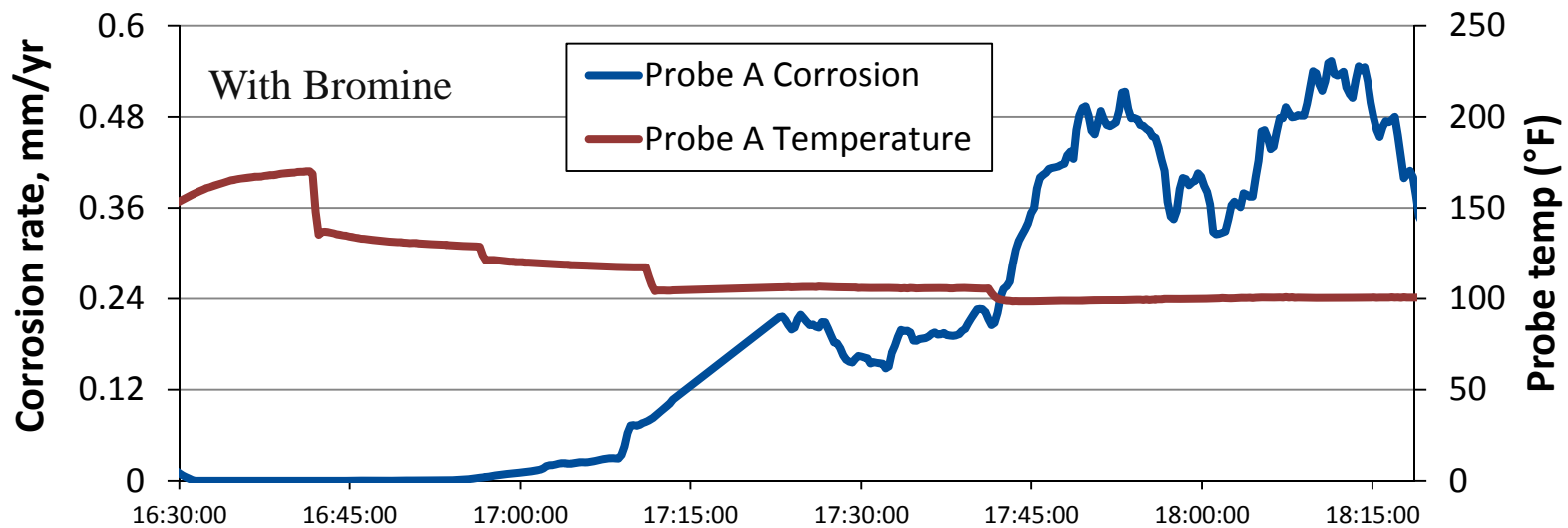
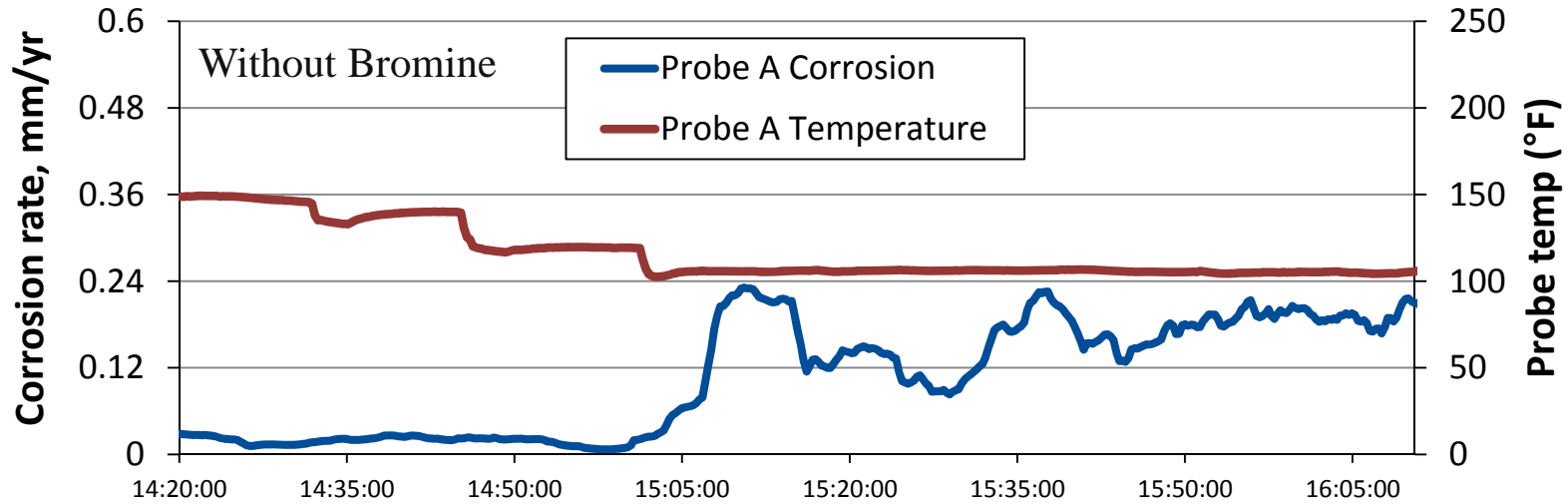
Carbon Steel Corrosion  
Sensor array  
(centered in flue gas duct)

Sensor surface temperatures were varied between  $\sim 350$  °F and  $\sim 100$  °F

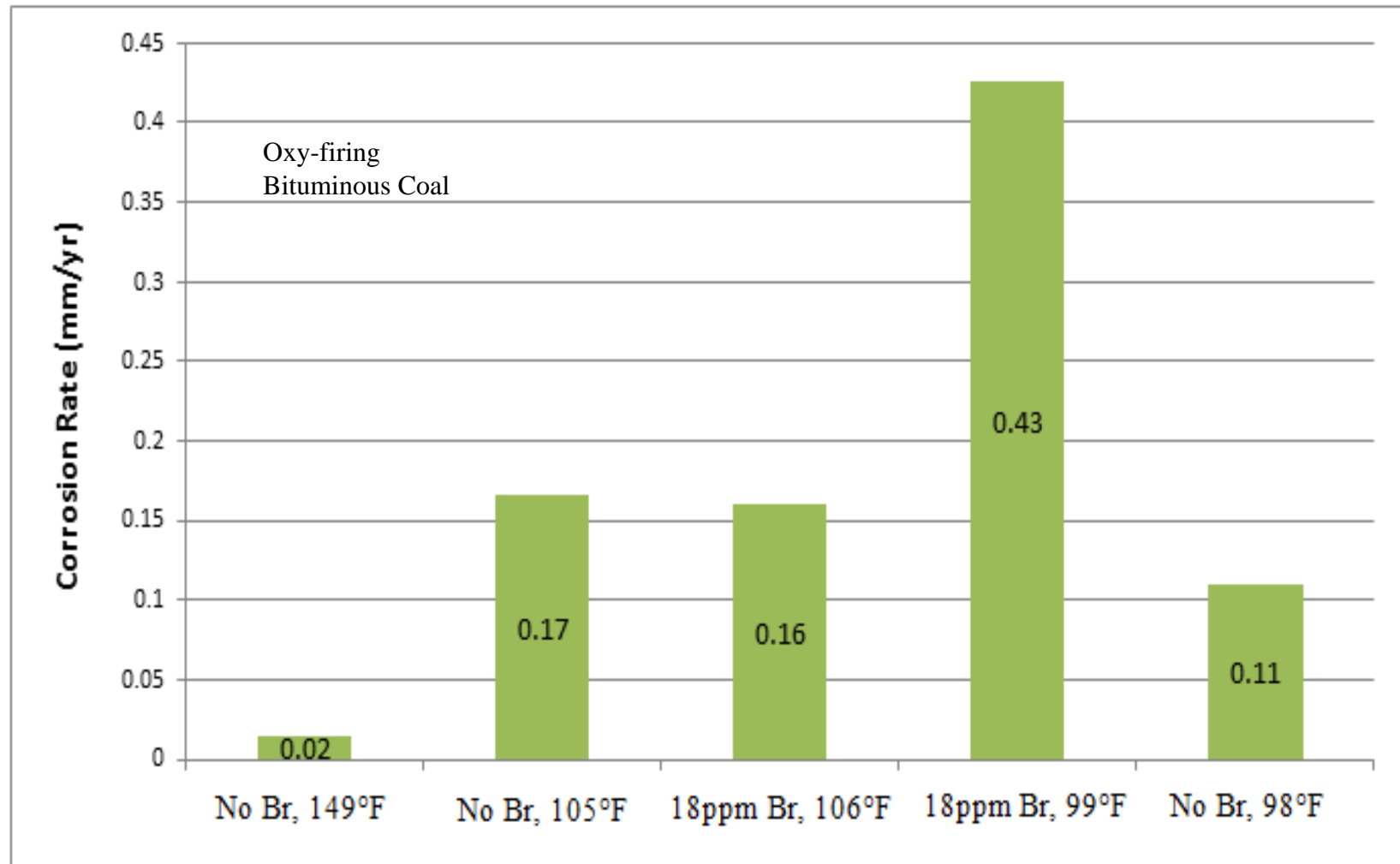
# Corrosion Rates (air-fired) (bituminous coal)



# Corrosion Rates (oxy-fired) (bituminous coal)



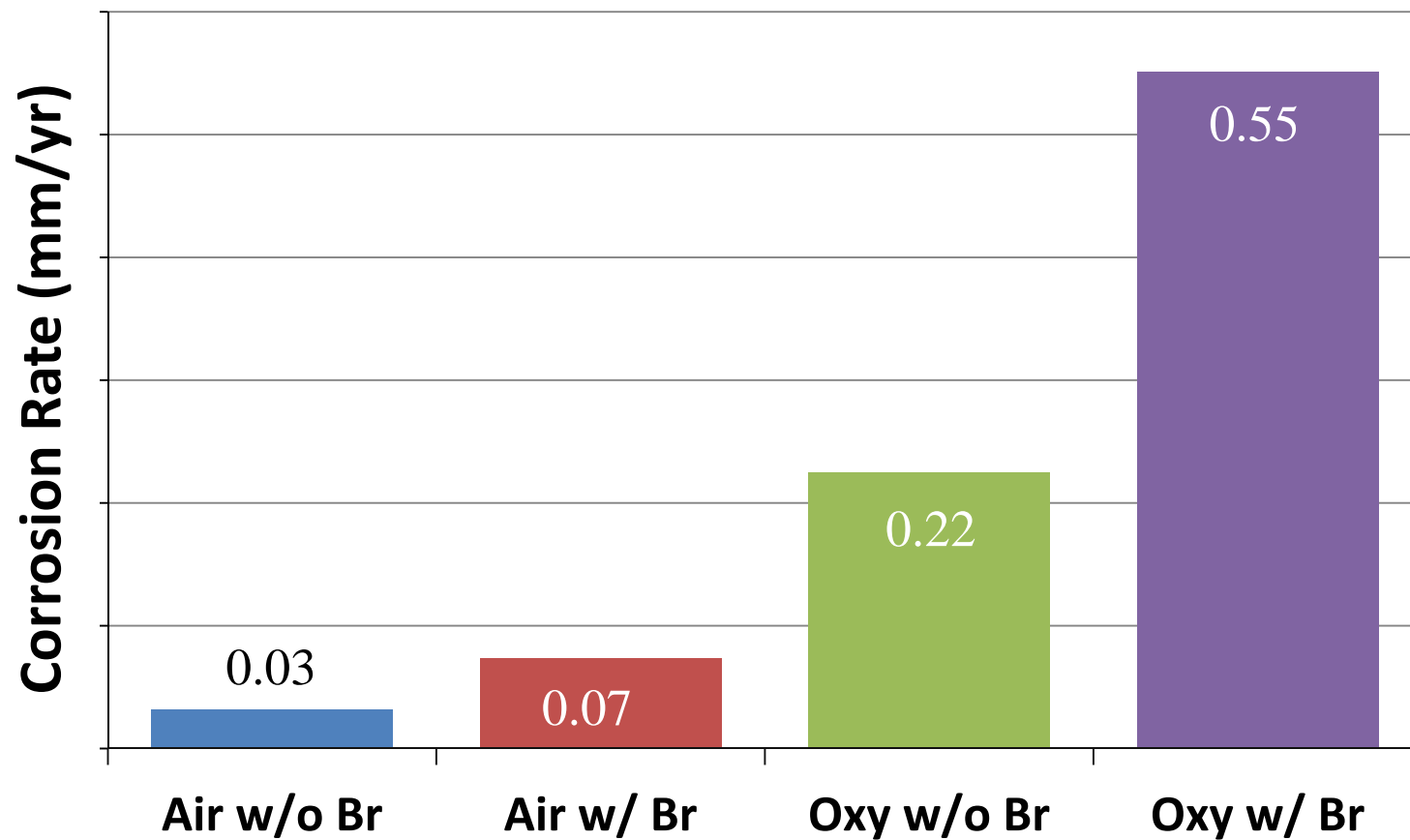
# Dew Point Corrosion Considerations



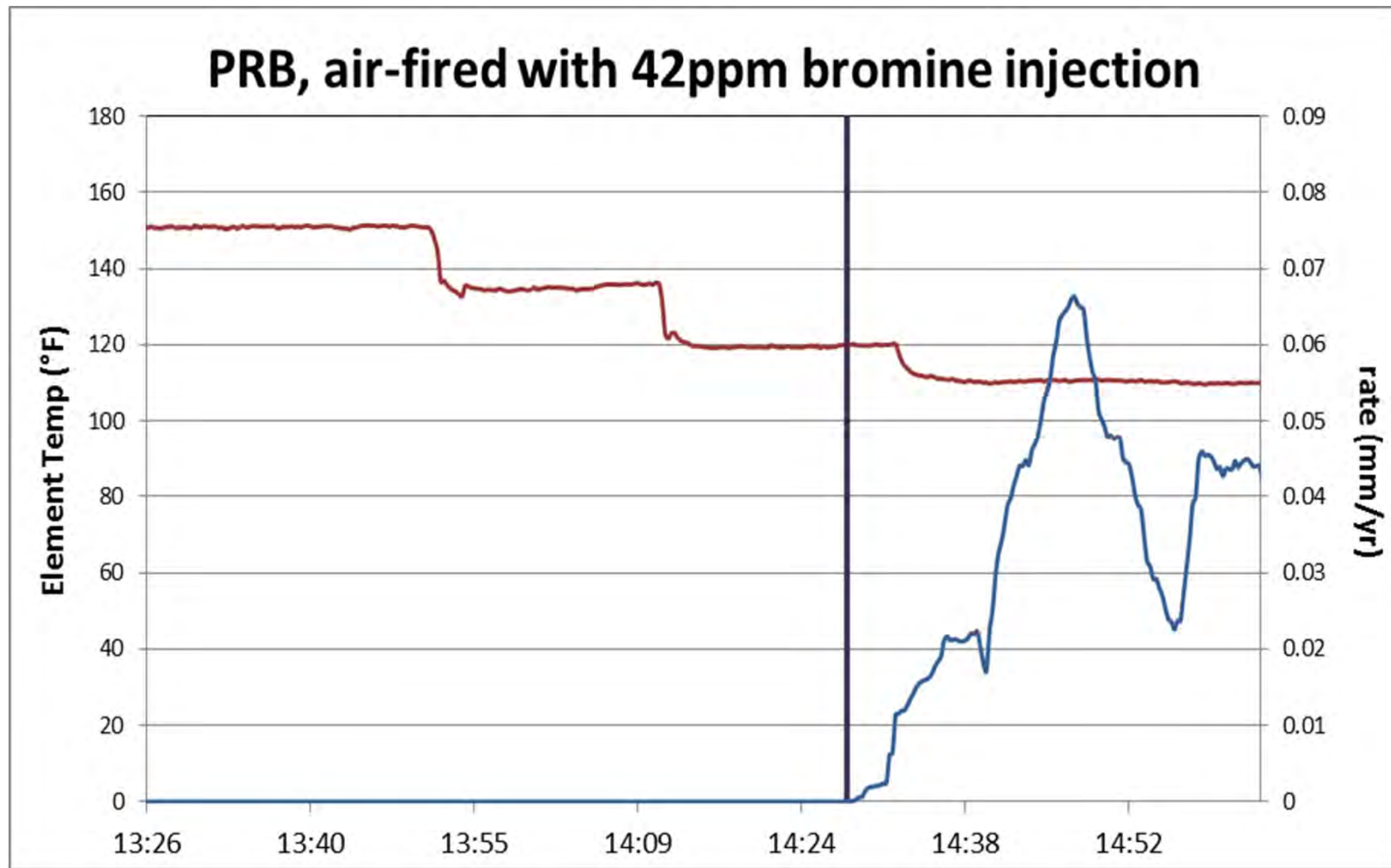
# Peak Corrosion Rates, bit. coal

---

---



# Dewpoint Corrosion with PRB



# Conclusions

---

- Corrosion rates at air heater temperatures can increase dramatically with bromine addition, if temperatures are sufficiently low
- Oxy-coal combustion has the potential to significantly increase air heater corrosion rates
- Dew point mechanisms are indicated and appear to involve sulfuric acid, HBr, HCl and water
  - ◆ Rates dependent on flue gas concentrations and moisture level (both higher with oxy-combustion)
- ACl appears to have a more complex impact on corrosion rates